nature portfolio

Peer Review File

Generalized and scalable trajectory inference in single-cell omics data with VIA

Reviewers' Comments:

Reviewer #1:
Remarks to the Author:
This manuscript proposed a trajectory inference method VIA, which is a graph-based approach utilizing lazy-teleporting random walks with MCMC refinement. In contrast to the single-cell graph based random walk methods, like DPT, the random walks of VIA are based on the cluster-graph so that it can reduce the time for pseudo-time inference and improve its robustness to different parameter settings. VIA does not make any assumptions on the trajectory structures so that it is flexible to characterize variety of topologies. Besides, the case studies of VIA on several real single-cell omics datasets along with validation of in-situ fluorescence image capture also valid the analysis. Overall, the paper is well written and provides sufficient supplementary details. I have the following questions and suggestions about the method and its applications to improve the manuscript.

VIA has been shown to be effective for rare branch detection, which implies, on the other side, it may also be sensitive to the data noises. How does its performance change with the increasing noise level of the data?
For graph edge accuracy, which is computed based on an F1-score. I think a false negative is: there exists an edge to connect to cell types that are not connected in the reference. Besides, since you compared VIA with Monocle3, PAGA, Slingshot…, what are the parameter settings of these algorithms? As the comparisons with other algorithms, you are supposed to search for many other parameters which may affect the performance apart from number of pcs and KNN. In the other experiments, this suggestion also holds true.
In Fig2.b, when you varied K in (KNN), the Graph edge accuracy of mnoncle3 is not changed. I wonder whether it is a true or not? Can you explain this?
In Fig3, if you would like to compare VIA with other algorithms under different number of pcs and KNN, a grid search of all the integers between 20-200 and 10-70 is more reasonable. Also, since the cluster are detected by PARC, I am interested in that whether the robustness to the number of pcs is mainly because of PARC, can you further confirm this?
In the experiment of E15.5 murine pancreatic cells, you said that 'VIA detects small endocrine Delta lineages and Beta subtypes'. Which part of the algorithm lead to this? PARC, or the lazy-teleporting MCMC?
For Fig7, since Slingshot is an algorithm that orders each single cell on the inferred cell lineage, while VIA just infers the trajectory of cell clusters. It seems unfair to compare these two algorithms considering time consuming.
VIA first represents the single-cell data in a k-nearest-neighbor (KNN) graph where each node is a cluster of single cells. However, VIA cannot infer the trajectories of single cells. Since the cell fate decision and changes of gene expression in single cells (especially the cells around bifurcation) are more important. Can the lazy-teleporting MCMC be applied to single cells in the PARC clusters to derive single cell trajectory?

Minor comments:
The 2D embedding plots of VIA and benchmarking methods in Figure 2 seem to be colored by different ways and the color legends are not displayed, which may be confusing.
The sizes in the figure texts are not unified and some of them are too small to read.
Fig1, caption, line84, 'can remain (orange arrows)' -> 'can remain Lazy (orange arrows)'
Fig2.a, M6 is missing on the first graph.

Reviewer #2:
Remarks to the Author:
The manuscript describes the development of a trajectory inference of large single cell datasets generated for example by scRNA-seq, imaging mass cytometry or imaging flow cytometry. There are a

plethora of algorithms that been designed to do exactly this task and the manuscript demonstrates advantages over a selection of these algorithms using a range of toy and real world data.

However this is a fast moving field and new algorithms appear almost monthly which appear to be capable of solving the same problems this approach is designed to be optimised for. For example how does this algorithm compare with

STREAM (Chen et.al. Nat. Comms, 2019) - which also compares performance with the algorithms benchmarked here and others such as scTDA, Wishbone, TSCAN,
SLICER, DPT, GPFates, Mpath, SCUBA which are not benchmarked in this work.

TinGa (Todorov et. al., BioInofrmatics 2020) - which appears to work well for the cycle and more complex geometries.

Tempora (Tran et.al. PLOS COMPUTATIONAL BIOLOGY 2020)

and these are to name just a few.

Also an example is given of the analysis of the cell cycle progress of cells using Imaging Flow Cytometry. However this type of analysis has been carried out previously (Blasi et.al. 2016, Eulenburg 2017 - Nat Comms) and the trajectory is not very complex so a simple diffusion map approach can work here.

The authors also use an ergodic approach (Kafri et.al.2013 Nature) to infer details about certain cell characteristics, however as Kafri discussed, care must be take to not use any predictor measure corrected to the response variable i.e. if you are inferring dry mass, volume then no correlated variables (e.g. cell radius, area etc) should be used in the pseudo time alignment.

I believe the manuscript is probably better suited to a method type journal as it appear to be an addition to an already large set algorithms to do this job and also the details of some of the examples need to be further elucidated as discussed above.

Reviewer #3:
Remarks to the Author:
1) This paper presents the VIA method for inferring trajectories in single-cell data, regardless of the –omics type. It relies on one metric, the F1-score (that assesses how accurately cell fates were identified by each method), to assess the accuracy of the VIA method and compare it to 5 state-of-the-art methods. This F1-score seems too weak of a metric to me, as it doesn't capture the structure of the returned trajectory. I can think of different trajectories (successively bifurcating, trifurcating, or even disconnected), that could have exactly the same cell fates, and thus return the same F1-score. I would thus recommend adding a second metric, next to the F1-score, that would capture the topology of the different trajectories. Moreover, the F1-score metric that was chosen by the authors doesn't allow them to compare all the tools that they included in the study (as PAGA doesn't automatically detect terminal states). If the paper chose to use only one metric to compare all methods, this metric should at least allow to compare all methods. In my opinion, the paper would benefit from adding at least one more metric to compare the methods on.

2) Small comment related to the previous one: in figure 2a), the authors state that the F1-score can't be computed for PAGA as this method doesn't automatically return cell fates. However, an F1-score was then computed for PAGA for the cyclic dataset (presented figure 2b), and disconnected dataset (presented in figure 2c). Please clarify in the text, in the methods, or in the description of figure 2 how and why the F1-score was computed for some datasets but not for others. The fact that the F1-scores

presented on the right of figure 2 correspond to a different set of methods for each dataset is confusing.

3) It is unclear to me why, in each figure where VIA is compared to other methods, it is not being compared to all the other methods. For example, why did the authors choose not to include the results of PAGA in figure 4? Of Monocle3 in figure 7?

4) The paragraph starting at line 378 should, in my opinion, be re-phrased. Historically, the first trajectory inference (TI) tools were designed to be applied on cytometry data (Wanderlust, Monocle). This type of data contains a much better ratio of cells over features than scRNA-seq data, and suffers less from sparsity, which typically makes it easier to find trajectories in this type of data. However, the way the paragraph is written now, the authors seem to suggest that most TI methods can only handle transcriptomic data, and that handling cytometry data would be a new advantage of VIA. I would thus advise to rephrase this paragraph to avoid misleading the reader.

5) The authors emphasize the fact that VIA doesn't require any user input parameters, compared to other methods. Only when reading the methods section do we discover that VIA needs the user to define a starting point to run. This should be stated earlier in the paper in my opinion (around line 25 for instance), as this is an information that any potential user of the method will be interested in. Side comment: as PARC allows a fast visualisation of the data, I'm wondering if allowing the user to choose a starting point in this representation of the data would be a nice way to simplify the choice of a starting point for the user.

6) The authors highlight the fact that the VIA method's computational advantage allows it to process larger amounts of dimensions, avoiding information loss due to dimensionality reduction. However, they test VIA on all original genes only in one dataset (presented in figure 4), and apply VIA on PCs for the other datasets. It would be interesting to see how the method performs on the original dimensions and how it compares to other methods on the synthetic datasets, and in figure 3.

7) Comment related to the previous one: it is surprising to see that VIA performs optimally when applied on > 6000 HVGs in figure 4, while Slingshot performs best on less than 2000 HVGs (which is more expected). This might be due to the fact that the F1-score captures only the accuracy of the end states recovered by the different methods, and doesn't represent differences in topology. It would be interesting to see whether the same increase in accuracy is observed when using more HVGs in the synthetic data and in figure 3.

REVIEWER #1 (Expertise: Trajectory inference, single cell data):

This manuscript proposed a trajectory inference method VIA, which is a graph-based approach utilizing lazy-teleporting random walks with MCMC refinement. In contrast to the single-cell graph based random walk methods, like DPT, the random walks of VIA are based on the cluster-graph so that it can reduce the time for pseudo-time inference and improve its robustness to different parameter settings. VIA does not make any assumptions on the trajectory structures so that it is flexible to characterize variety of topologies. Besides, the case studies of VIA on several real single-cell omics datasets along with validation of in-situ fluorescence image capture also valid the analysis. Overall, the paper is well written and provides sufficient supplementary details. I have the following questions and suggestions about the method and its applications to improve the manuscript.

R1.Q1 VIA has been shown to be effective for rare branch detection, which implies, on the other side, it may also be sensitive to the data noises. How does its performance change with the increasing noise level of the data?

R1.A1 We thank the reviewer for this question and have investigated the impact of noise on VIA's performance. We first wish to point out that a good indicator of VIA's robustness to noise is that it works well on a wide range of real complex datasets, spanning various numbers of lineages, population abundances and wide ranges of feature and cell counts. In particular, a trait common to all scRNA-seq datasets is the high level of "drop-out" or zero-inflation of counts, which in turn intensifies challenges related to high dimensionality and unbalanced size in rare and abundant cell types (P. Qiu 2020). To conduct a more focused study on the impact of noise, we have added the following section in **Supplementary Note S4** , " **Noise and drop-out in scRNA-seq data** " to the Supplementary Information:

"We use the R package "seqgendiff" (Gerard, 2020) to add noise to the real RNA-seq datasets to intensify the attributes of noise in real data. Seqgendiff uses binomial thinning to subsample counts using the binomial distribution and reduce the total count expression by a specified factor. Before applying binomial thinning, seqgendiff randomly selects a subset of the original features (genes) so that the results are not dependent on the behaviour of a few features (genes).

We first show the deterioration in VIA's inferred topology for a synthetic 4-leaf multifurcation ***(Fig. S17)*** *, when the level of noise is increased (or the signal strength is diminished) by a factor of 2 at each step. Note that prior to binomial thinning, only 10% of the original features are retained (at random) from the original input to mitigate dependency on a few select features. Since the signal in the synthetic data is strong, we can recover the overall multifurcating topology and delineate 3-4 of the 4 cell fates until a noise-factor of around 5. At higher levels of signal atrophy (Factor 7 and 8), the true structure is imperceptible.*

To show the impact of adding noise to a real dataset (such as the endocrine dataset where the Delta lineage is very small, and the Epsilon lineage is easily merged with the Alpha islet cells), we compare VIA to other methods in terms of the inferred topology and predicted gene trends which are computed based on the single-cell level lineage probabilities and cell ordering. ***Fig. S18b-c*** *UMAPs illustrate the level of added noise showing the separation between lineages becoming obscured in the noised-data visualization. A thinning factor = 1 was used on 25% of genes as adopted in Gerard 2020 and the package vignettes. VIA's inferred trajectory remains true to the expected progression from endocrine progenitors, then to a forking at the Fev+ intermediate state towards different islets. More importantly, STREAM, Slingshot and Palantir appear to suffer most from the added noise as seen by the high 'cross-talk' between the plotted lineage trends (e.g. in the Palantir and Slingshot trends), or the detection of only two islets (e.g. Palantir), or in the case of STREAM the compromised topology where Alpha/Beta cells are plotted along the same branch, and the Epsilon/Delta are likewise combined."*

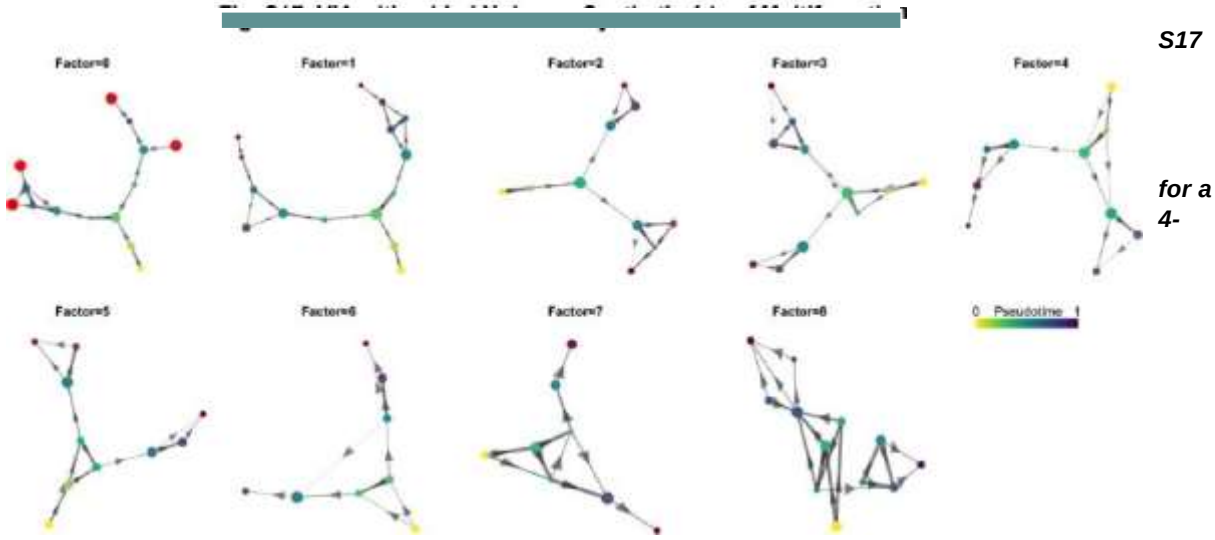

Fig. S17 ***Impact of noise on VIA's inferred topology for a synthetic 4-leaf multifurcation.*** *Noise is added using R package "seqgendiff". 10% of the original 1000 features are sampled and retained. Then binomial thinning is applied where the aggregate signal is lowered to* $^{2-factor}$ *its original strength.*

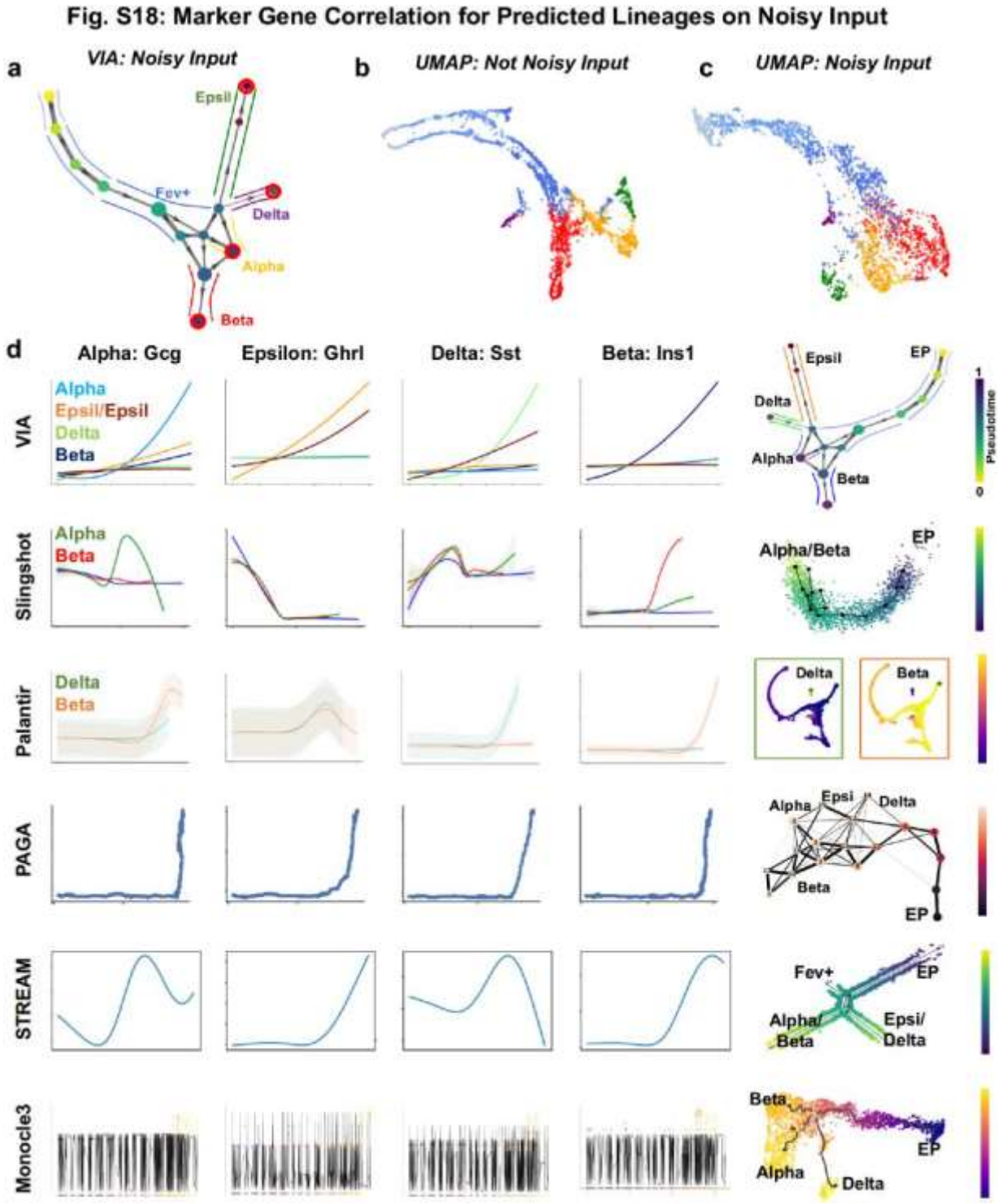

136 ***Fig. S18 Gene correlation for predicted lineages on the "noised" pancreatic endocrine dataset.*** *25% of quality*
137 filtered genes are retained, followed by factor 1 binomial thinning ***(a)*** *VIA topology for noised input shows the desired*
138 progression of cells through 2 channels of Fev+ cells towards automatically identifying the 4 islets (red circles). ***(b)***
139 UMAP of original input ***(c)*** *UMAP after applying binomial thinning blurs boundaries between the islets* ***(d)*** *comparison*
140 of inferred topology and gene trends shows that many methods merge lineages together and fail to detect 4 distinct
141 islets corresponding to the Alpha, Beta, Delta and Epsilon lineages

R1.Q2 For graph edge accuracy, which is computed based on an F1-score. I think a false negative is: there exists an edge to connect to cell types that are not connected in the reference.

R1.A2. We thank the reviewer for the enquiry into the F1-score pertaining to graph edges. The F1-edge score is defined as follows: A false negative edge in the inferred model is when there is an edge in the reference model connecting clusters/cell types/groups that is absent in the inferred trajectory. A false positive edge in the inferred model is when an edge occurs in the inferred model that is not actually present in the reference model. A true positive edge is one that exists in the inferred model that also exists in the reference. These three measurements are used to compute the F1-score.

$$F_1 = \frac{tp}{tp + 0.5(fp+fn)}$$

R1.Q3 In Fig2.b, when you varied K in (KNN), the Graph edge accuracy of monocle3 is not changed. I wonder whether it is true or not? Can you explain this?

R1.A3. For this particular dataset, the trajectory inferred by Monocle3 did not change with respect to the value of K in KNN. Sample outputs for Monocle3 on this cyclic dataset (**Fig. S3c)** do not change in terms of the milestones or edges and therefore result in the same F1-score. This is driven by the invariance of the UMAP components for this dataset, which is the input to the clustering and subsequent TI.

To elaborate further on the question of Monocle3's behaviour to changing K, we often found that Monocle3's inferred trajectory did not necessarily reflect increased connectivity for higher K, or conversely, diminished connectivity for lower K. For instance, in all the disconnected synthetic datasets, Monocle3 tended to add edges between disconnected components. We found that decreasing K did not reliably alleviate this problem. However, we rather surprisingly found that for several of the real datasets which we know have a common precursor cell type (e.g. Pancreatic endocrine progenitors, hematopoietic stem cells), the lineage specialized cells would be disconnected from the main body of early and intermediate state cells, and thus unreachable from the progenitor cells. We could not reliably encourage connectivity by simply increasing K. As such we found that the "super groups" implied by Monocle3 do not necessarily imply truly disconnected trajectories. This suggests that perhaps the highly connected trajectory of the MOCA 1.3 Million cells revealed by VIA offers more information about the progressive specialization of cells, compared to the Monocle3 interpretation which offers a more disconnected and clustered view **(Fig. 7)** .

R1.Q4 Besides, since you compared VIA with Monocle3, PAGA, Slingshot..., what are the parameter settings of these algorithms? As the comparisons with other algorithms, you are supposed to search for many other parameters which may affect the performance apart from the number of PCs and KNN. In the other experiments, this suggestion also holds true.

R1.A4. We thank the reviewer for their question regarding the choice of parameters in the benchmarked methods. We agree there are often several parameters left to the choice of the user, with some of these parameters only becoming apparent after various tests and runs, as some parameters tend to be 'under-the-hood'. To address this question, we have added two tables in the Supplementary Information outlining the choice of parameter settings and when or why we chose a non-default setting: The new **Table S4** summarizes the parameters selected for each dataset that were then further investigated to observe impact on performance. The new **Table S5** summarizes the choice of parameter settings for each method.

In general, our approach was to follow the approach shown in tutorials (Jupyter NB) of other methods which recommend parameter settings and in some cases indicate how to deviate from default parameters. In general, we found KNN and/or PC to be key parameters common to all methods and therefore chose to focus our benchmarking on these.

Process	Type	Dimensions	Starting Point	Range of parameters varied	Remarks
Synthetic	DynToy	1000 cells x 1000 features	M1 (Milestone 1)	K-NN=20, PC=10 for composite accuracy	Each composite score comprises 5 metrics and thus we fixed the number of KNN and PCs for calculating the composite accuracy of synthetic data
Hematopoeisis	scRNA-seq	5500 cells x 14651 genes	HSC	K-NN={10,20,...,80} PC ={10,20,...,200}	Both knn and PC are varied to conduct a more comprehensive gridsearch
Hematopoeisis	scATAC-seq	2034 x 8192 TF	HSC	K-NN=20 PC = {10,20,...,200}	We consider the results for two different pre-processing pipelines and limit the parameter range to only varying the PCs
Pancreatic	scRNA-seq	2531 x 10,000 ?? genes	Endocrine Progenitor	HVG = {300,500,1000,2000,...,10000} PC = {30,40,...,80}	Here we primarily consider the effect of varying the number of HVGs
MOCA	scRNA-seq	1.3 Million Cells	E9.5 Epithelial cell	K-NN={20,30,...,50} , PC = {30} PC = {20,30,...,50}, KNN = {30}	We visually compare outputs of methods that are able to process this dataset within 3 hours
Cardiac	scRNA-seq/ scATAC-seq	695 cells+ 197 cells	Cardiac Progenitor	K-NN=10 (knn=15 for Palantir which otherwise fails at lower knn=10)	Here we primarily consider the effect of varying the number of PCs. K (KNN) is set to a low value since the the cell count is small
mESC mesoderm	CyTOF	90,000 cells x 28 antibodies	Day 0 cell	All features used w/o PCA, except Slingshot which could not handle the full-feature set at high cell counts K-NN = **{10,20,30,...,}**	Sample time annotations allow us to compute pseudotime correlations for this dataset for different K values using all 28 antibodies directly (except Slingshot which required PCA to handle the high cell count)
Cell cycle	Imaging	4000 cells x 38 morphological features	G1 cell/ G1 cluster	All features are used K-NN=20	The 38 features (without PCA) are run directly. Subsets of these features (e.g. excluding volume related features) are probed

Table S4: Summary of key parameters considered in benchmarked datasets. *In particular, the table also summarizes the choice of root (i.e.starting point of the trajectory) and the rationale for which parameters are probed to impact TI for each dataset.*

Method	General Parameter settings with emphasis on why/when parameters are changed from default	Starting point selection
VIA	• Underlying PARC settings were left at default graph pruning and Leiden resolution. • We showed that good results are achievable using other clustering such as kmeans (n_clusters set to 20 as a default) which shows that the VIA method is not overly dependent or sensitive to clustering methods, as long as a sufficient resolution is captured.	Provided as a single cell index corresponding to an early cell for real datasets; provided as a group-level label for more data-driven starting point selection for Synthetic data where Milestone group annotations are available
PAGA	• Set the number of KNN for both the PCA and diffusion map iteration • The number of PCs and diffusion components in both knn-graph stages is set to the number of PCs selected rather then allowing the diffusion components to be subset to the default 10 DCs • To plot gene trends we need to manually select appropriate terminal clusters and then manually select a corresponding set of clusters that make up a lineage-pathway	A single cell index corresponding to a suitable early cell (the same starting cell is given to all methods requiring a single-cell root)
Slingshot	• KNN is not a parameter in Slingshot and hence not 'grid searched'. • We first tested the method using the recommended GMM clustering but found this to be too coarse to detect the relevant lineages. The other option was using KMeans where we typically set K=15 to allow for slight overclustering without adding too much fragmentation. Slingshot's visualization of lineages is linked to the input PCs which makes it difficult to visualize results on more complex data where 2 PCs are not a good basis for visualization.	Root manually selected as the cluster containing HSCs and the 'start' of the trajectory
Monocle3	• Monocle3 requires UMAP to be applied to the PCs before computing TI. This is recommended on their tutorial pages as part of their intended pipeline and also prompted by the tool when running it. As such, the KNN is set as the number of neighbors used in the UMAP computations and the PC value is the number of top PCs used as UMAP input. • The default distance metric set by Monocle in using UMAP is "cosine distance" but this works very poorly for the datasets at hand and we therefore switched to Euclidean distance which significantly improved results	Root branch is manually selected after getting the branching structure and selecting the most suitable milestone based on the ground truth annotations of early cells (progenitors, stem cells)
STREAM	• For STREAM, the original use case suggests to run PCA followed by one of UMAP, MLLE or Spectral Embedding (SE). To ensure consistency in benchmarking and reduce the impact of additional feature reduction and subsetting incurred by a second stage of dimensionality reduction, we chose to only perform the PCA step and skip further dimensionality reduction (a more detailed explanation is given below). • SE was generally too coarse for complex real data (often yielding a simple bifurcation) and MLLE tends to overfragment the data such that almost each cell type (early, intermediate and late) corresponds to a "leaf branch". MLLE was thus sensitive the number of components retained and quickly reached a breakpoint where overfragmentation occured. UMAP, like SE, was often too coarse and limited the granularity. • Due to the uncertainty introduced by choice of secondary Dimension reduction (with no clear winner), we choose to apply only PCA and skip the second dimensionality reduction step. This also makes for a fairer comparison to palantir, paga, Slingshot and VIA which are computed on the PCs. • For the Cardiac scATAC-seq /scRNA-seq datasets, Stream would not run on the PCs (i.e. produced errors) so we used SE after PCA. • We follow the tutorials provided by STREAM to incorporate a two stage approach suggested for more complex data. This allows you to refine the graph by adding more branches and nodes in a second iteration. • All other parameters such as the number of initial clusters, the incremental clusters used in intializing and seeding the graph, were left as default (as per the tutorial). • KNN is not a relevant parameter unless SE/UMAP/MLLE are used.	Root branch is manually selected after getting the branching structure and selecting the most suitable branch based on the ground truth annotations of early cells (progenitors, stem cells)
Palantir	• Set the number of PCs and KNN in run_diffusion_maps() and run_pca() function and override the default PC and KNN settings which otherwise subset the DCs to 10. • The number of sampling points is left at the default 1500 as Setty et al., 2019 show robustness to this parameter	A single cell index corresponding to a suitable early cell (the same starting cell is given to all methods requiring a single-cell root)
CellRank	Ran as shown on the tutorial page to reproduce the results shown in their paper for endocrine data. Skipped for other datasets as they did not have unspliced counts	Automatically determines the starting point. Since this would sometimes incur spurious starting points, we compared gene trends of the pancreatic dataset for an output which detects the correct root.

Table S5: Summary of settings selected for benchmarked methods. *Method-specific parameter settings and rationales for non-default choices are provided for each of the benchmarked methods.*

R1Q5. In Fig3, if you would like to compare VIA with other algorithms under different numbers of PCs and KNN, a grid search of all the integers between 20-200 and 10-70 is more reasonable.

R1.A5. The suggestion to make the stress-tests more comprehensive and uniform across methods and datasets is well received. In the revised manuscript, we added a new systematic benchmarking that ensures regular increments along the number of PCs or KNN and also included Monocle, PAGA (whenever possible) and STREAM in all benchmarking analyses across datasets (as highlighted in our response to Editor's comment) . In new **Table S5** we further explain which parameters are varied (i.e. KNN, or PC, or HVGs) and why we consider a particular set of parameters for different datasets.

R1.Q6. Also, since the clusters are detected by PARC, I am interested in whether the robustness to the number of PCs is mainly because of PARC. Can you further confirm this? In the experiment of E15.5 murine pancreatic cells, you said that 'VIA detects small endocrine Delta lineages and Beta subtypes'. Which part of the algorithm leads to this? PARC, or the lazy-teleporting MCMC?

R1.A6. We thank the reviewer for this interesting question regarding the dependency of VIA's lazy-teleporting random walks on PARC, to robustly delineate rarer but distinct cell types. We have analyzed this further, and the reviewer is also invited to read the response to Editor (Point # **3).** We added a new section investigating this issue in the **Supplementary Note S6 ,** which the reader is also referred to from the Methods section (" **VIA Algorithm** ") pertaining to the clustering step:

" *If the user prefers another clustering method or has group-labels of cell types according to apriori information, VIA can easily accommodate such a substitution and the robustness of the lazy-teleporting random walks to different clustering approaches is shown in* ***Supplementary Note S6 and Fig. S30-S32*** *for both real and synthetic data"*

As also explained in ***Supplementary Note S6*** :

"A key step in VIA is to reduce the single-cell graph into a cluster-graph using the PARC's community detection algorithm. We assessed the performance of VIA when substituting PARC with another clustering method (in this case we chose Kmeans as it is *representative of extremely simple but fast clustering) to show that VIA's teleporting-random walks still traverse and uncover the expected trajectories and their associated lineage-cell-fates.*

The analysis shows two key characteristics, the first is that VIA's performance is not limited to using PARC in the clustering step (***Fig. S30a*** *), and the second is that given the continuous nature of the underlying synthetic data (* ***Fig. S30b*** *), VIA's lazy-teleporting random walks still work well even when the data is not inherently highly clustered. We first tested performance on the synthetic datasets and compared the composite metric scores of VIA with PARC and with Kmeans. The composite score allows us to quantify accuracy of topology, pseudotime and F1-cell fate prediction for all synthetic datasets across various topologies and demonstrate that VIA using Kmeans yielded competitive results* ***(Fig. S30a).***

Following this, we also show that the expected gene trends and progression of cells can be recovered on real data (scRNA-seq hematopoiesis and endocrine genesis). In ***Fig. S31-S32*** *, we not only show that the topology uncovered remains true to the known biological progression towards committed lineages (as verified through reference to literature of the hematopoietic and endocrine genesis processes), but also that the gene expression trends of known marker genes plotted versus the inferred pseudotime for each of the predicted lineages, reflect the expected upregulation. We set 20 as the number of clusters, however, at n=10 clusters, the megakaryocyte cells are absorbed into the larger erythroid lineage, and the dendritic cells are merged together or at times even absorbed into the monocytic lineage).*

Thus, a drawback of using Kmeans is that the choice of number of clusters needs to be sensible to capture the desired resolution. In a classical clustering scenario, this might be more problematic as the choice of

number of clusters can incur fragmentation of cell types in order to uncover a smaller population, thus generating 'false clusters', or merging of dissimilar cell types if the number of clusters is set to be too low.

To avoid the issue of setting the number of clusters, methods like PARC uncover the underlying granularity in a data-driven manner (without requiring a predetermined number of clusters). In PARC, the underlying graph pruning allows it to automatically detect rarer cell types. However, for the datasets considered, we found that setting K to a sensible number that captures populations of various abundances along the trajectory, still allows the relevant neighborhood information to be subsequently propagated in the random walks. These results ultimately allow the user more flexibility in their choice of how to group or cluster cells or potentially even use prior knowledge of cell types to guide the inferred trajectory."

Fig. S30: VIA robust to choice of clustering method

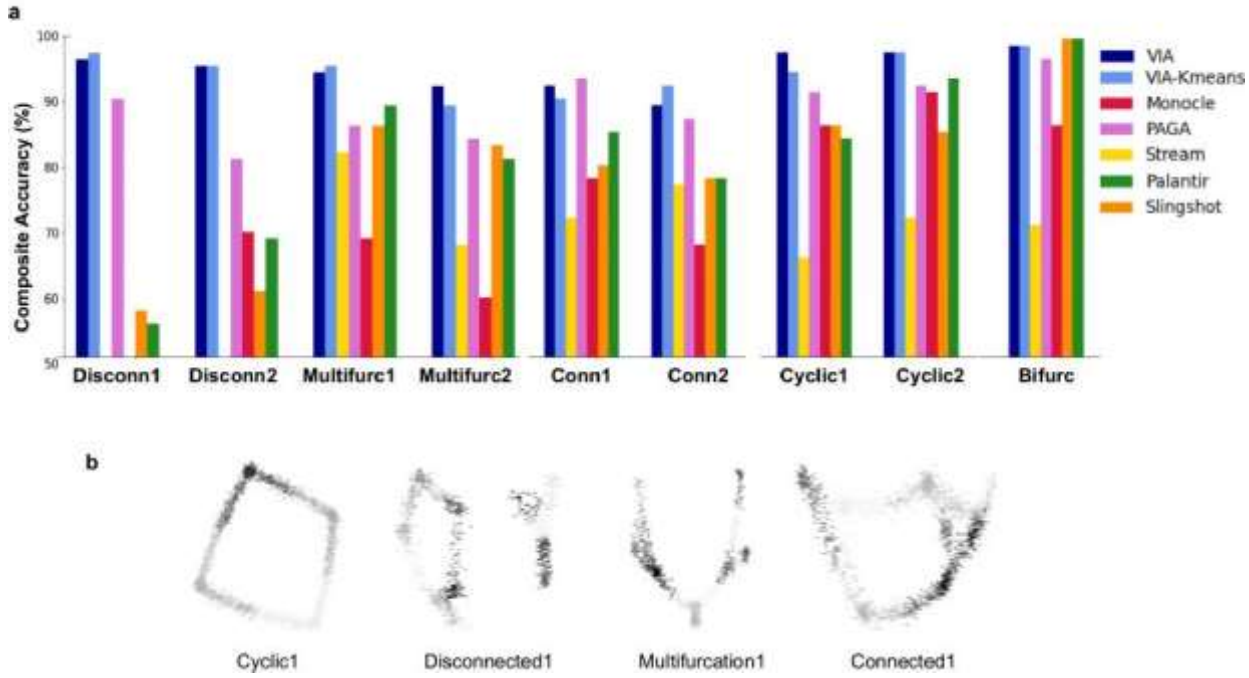

Fig. S30 VIA with Kmeans clustering in lieu of PARC in the clustering step of VIA for synthetic data maintains accuracy of TI (a) *VIA with Kmeans (VIA-Kmeans) and the original VIA, i.e. VIA with PARC, (VIA) are comparable in terms of performance on synthetic datasets, with both approaches maintaining a competitive advantage over other methods, particularly for multifurcations and disconnected and connected topologies* ***(b)*** *Synthetic datasets plotted with first two principal components show the underlying data is continuous and not composed of discrete clusters.*

Fig. S31: VIA using KMeans on Pancreatic Islets

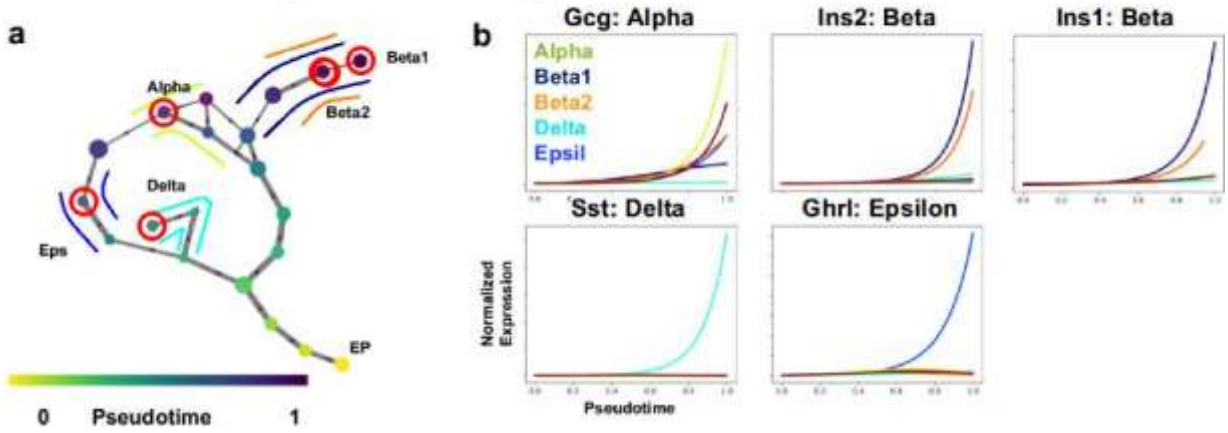

Fig. S31 VIA with Kmeans clustering in lieu of PARC for endocrine genesis data (a) *At 20 clusters, VIA automatically detects the 4 islets as terminal states (red circles). The topology captures the progression of lineage commitment arising after progressing from Ngn low to high EPs, followed by intermediate Fev+ cells.* ***(b)*** *unsupervised gene expression vs. pseudotime of lineage markers show the unique elevation of specific genes with minimal cross-talk from unrelated lineages. The two Beta subtypes are detected, with the Beta-2 subtype expressing Ins2 but not Ins1*

Fig. S32: VIA using KMeans on scRNA-seq Hematopoiesis

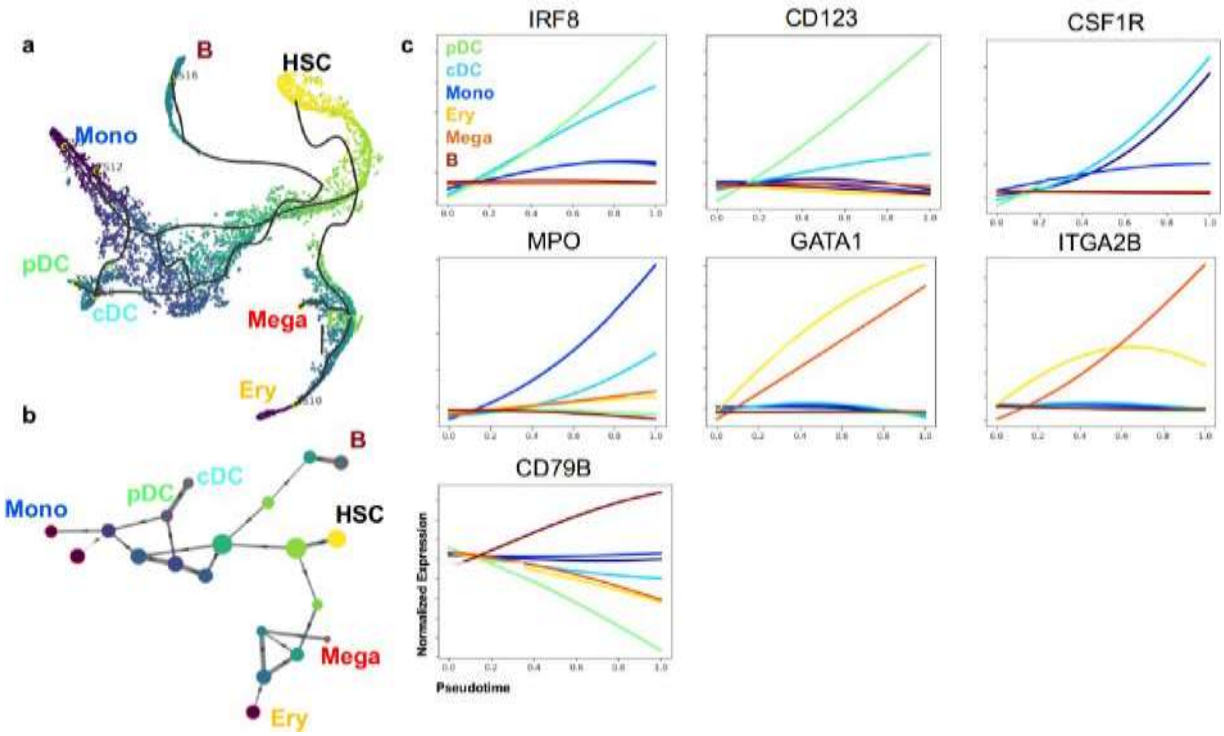

Fig. S32 VIA with Kmeans clustering in lieu of PARC for scRNA-seq Hematopoiesis (a) *At 20 clusters, VIA automatically detects the 6 lineages specific to the pDC, cDC, Monocyte, Megakaryocyte, B cell and Erythroid cell fates* ***(b)*** *unsupervised gene expression vs. pseudotime of lineage markers show the unique elevation of specific genes with minimal cross-talk from unrelated lineages. Notably ITGA2B (CD41) is elevated in the Megakaryocyte lineage and CD123 is elevated in the DC lineage representing the pDCs, and CSF1R is elevated in the cDC lineage*

R1.Q7. For Fig.7, since Slingshot is an algorithm that orders each single cell on the inferred cell lineage, while VIA just infers the trajectory of cell clusters. It seems unfair to compare these two algorithms considering time consumption.

R1. A7. We would like to take this opportunity to clarify that although VIA begins by reducing the single-cell graph to a cluster-level graph, VIA also ultimately provides a single-cell level pseudo-temporal ordering and single-cell level lineage-association probability which is used to plot the lineage-pathway and gene trends towards each individual predicted cell-fate. The projection of VIA's inferred results to a single-cell level is included in the reported runtimes. We have now made this clearer within the main algorithm description of the main text as follows:

*" The single-cell level KNN Graph constructed in **Step 1** is used to project the lineage probabilities and temporal ordering derived from the cluster-graph topology onto a single-cell level. Together, these four steps facilitate holistic topological visualization of TI on the single-cell level (e.g. using UMAP or PHATE [14,15]) and critically enable data-driven downstream analyses such as recovering gene expression trends and single-cell level pathways of lineages, that are essential to biological validation and discovery of lineage commitment (**Methods**) (**Step 5 in Fig.1**)."*

We note that Slingshot's first stage of TI constructs an MST on the clusters of cells to delineate lineages of clusters. These lineages are then used to construct principal curves, where the pseudotime of a cell is the arc distance along a curve from the root. (Street et al. 2018). Thus, the single-cell level lineage association probabilities and pseudotimes of VIA and Slingshot offer comparable levels of resolution.

In the main text, we typically show the graph-level trajectory as this often succinctly summarizes the overall topology and does not require an additional step and choice of manifold embedding. However, notable examples of the single-cell values of pseudotime ordering are shown in **Fig. 6b-c** where the 1.3 million cells of MOCA are colored by the VIA inferred single-cell pseudotime , and the single-cell probabilistic lineage pathways for different lineages within the major groups are shown in **Fig.6c** . In the case of MOCA we projected the results onto the PHATE embedding, but the embedding method can be chosen by the user and the single-cell level values of VIA are independent of the type of visualization algorithm. Note that the cytometry datasets (CyTOF of 90K cells and FACED images of 3000 cells) are also displayed at both the graph and single-cell levels in **Fig. 7a** and **Fig. 8c,e.** Additionally we show the single-cell temporal ordering and lineage pathways for other endocrine and hematopoietic datasets in **Fig. S7, S10, S13, S14 and S19** .

R1. Q8. VIA first represents the single-cell data in a k-nearest-neighbor (KNN) graph where each node is a cluster of single cells. However, VIA cannot infer the trajectories of single cells. Since the cell fate decision and changes of gene expression in single cells (especially the cells around bifurcation) are more important. Can the lazy-teleporting MCMC be applied to single cells in the PARC clusters to derive single cell trajectory?

R1.A8. We thank the reviewer and think there are a few facets to this question. First, as we clarified in our previous response (**R1.A7**), VIA does offer a single-cell level temporal ordering that can be used to analyze the gene trends along pseudotime at the single-cell level. Second, the granularity of the cluster-level graph is also easily controlled using the resolution parameter. The underlying cluster-graph also makes VIA readily access much larger datasets where the global topoglocial picture can be obscured at a single-cell level. Third, since we are able to extract single-cell lineage and temporal ordering of cells using the properties of the cluster-graph and neighborhood information of the original single-cell graph, we can perform unsupervised prediction of key gene changes beyond up/down regulation, and even infer more subtle changes like the slow-down in the S-phase of cell growth in the cell cycle of FACED-image-based cytometry features; predict the synchronized upregulation of GATA1 in the erythroid lineages, accompanied by the suppression of the GATA2 gene; recover different rates of change of gene expression in the pre-B cell differentiation **(Supplementary Fig. S6)** which closely mirror the reference expression levels which are annotated by sampling time (in hours).

While in theory it would be possible to simulate the lazy-teleporting random walks at single-cell level, it would be impractical to extend the method to this level in terms of the computational cost and runtime. Throughout our manuscript, the tests on our datasets have shown that the cluster-graph approach does not sacrifice accuracy in terms of revealing accurate topology, cell fates and analyzing the gene/feature trends of cells ordered at the single cell level. Moreover, global relationships are better retained at the cluster-graph level, which is key to interpreting massive datasets like MOCA.

Minor comments:

R1. Q9. The 2D embedding plots of VIA and benchmarking methods in Figure 2 seem to be colored in different ways and the color legends are not displayed, which may be confusing.

R1.A9 *Thank you for pointing this out, we have now added legends for the different outputs to guide the reader.*

R1. Q10. The sizes in the figure texts are not unified and some of them are too small to read.
Fig1, caption, line84, 'can remain (orange arrows)' -> 'can remain Lazy (orange arrows)'
Fig2.a, M6 is missing on the first graph.

R1.A10. Again, thank you for pointing this out, we have amended these typos accordingly too.

REVIEWER #2 (Expertise: Cell cycle analysis using flow cytometry data):

The manuscript describes the development of a trajectory inference of large single cell datasets generated for example by scRNA-seq, imaging mass cytometry or imaging flow cytometry. There are a plethora of algorithms designed to do exactly this task and the manuscript demonstrates advantages over a selection of these algorithms using a range of toy and real world data.

R2. Q1. However this is a fast moving field and new algorithms appear almost monthly which appear to be capable of solving the same problems this approach is designed to be optimised for. For example how does this algorithm compare with

- *STREAM (Chen et.al. Nat. Comms, 2019) - which compares performance with the algorithms benchmarked here such as scTDA, Wishbone, TSCAN,SLICER, DPT, GPFates, Mpath, SCUBA which are not benchmarked in this work.*
- *TinGa (Todorov et. al., BioInformatics 2020) - which appears to work well for the cycle and more complex geometries.*
- *Tempora (Tran et.al. PLOS COMPUTATIONAL BIOLOGY 2020)*

R2. A1. We thank the reviewer for their suggestion to consider other methods that have also been developed with the aim of achieving complex trajectory inference. We selected the methods we benchmark based on strong performance in a recent benchmarking analysis (Saelens et al. 2019) as well as certain prerequisites shown to be satisfied within their papers, i.e. the ability to automatically predict cell fates and lineages on non-tree topologies, scale to large number of cells and even handle various omic data types (i.e. Palantir, Slingshot, Monocle3). We note that although PAGA does not provide automated cell fate prediction, its scalability and flexibility with regards to topology and single-cell modalities, and the ability to integrate DPT to extract single cell pseudotime, make it largely relevant to our analysis. Here we outline our rationale for choosing whether or not to include STREAM, TinGa and Tempora:

STREAM (Chen et al., 2019): We have now included STREAM in our benchmarking analysis for all datasets (real and synthetic) across all stress-tests. STREAM offers pseudo temporal ordering and cell fate lineage prediction on real datasets and can be included in most of the comparative analyses within our paper. We note that the methods Chen et al., chose to benchmark in their paper all performed significantly worse in the Saelens et al. 2019 benchmarking study, than the methods we already included in our paper. It focuses on tree-like trajectories and also lacks scalability (taking 4 hours on high-dimensional data of 500 features and 2000 cells, and over 6 hours on high cell count of 1 Million MOCA cells of 30 PCs).

TinGa (Todorov et al, 2020): While TinGa is an interesting new method, it does not predict cell fates or lineage pathways which we view as an essential part of real-data analysis to facilitate unsupervised analysis of lineage committed cells, the differentiation pathways and the gene expression along their respective lineages. Without this information, TinGa would require manual setting of cell fates and the associated lineage pathways in order to be included in the benchmarking conducted on the real datasets in our paper. We also noticed that Todorov et al.'s testing of real data is generally limited to smaller and simpler scRNA-seq datasets. As such, STREAM appears to be better suited to the benchmarking framework used in this paper.

Tempora (Tran et al., 2020): This is also an interesting tool but is tailored to transcriptomic data which (preferably) have temporal annotations that can be used to guide the trajectory. Tempora is also designed to incorporate Gene Ontology terms to create a pathway enrichment profile which removes redundant pathways. Tran et al., show that without the use of GO terms - which would be the case for non transcriptomic data - the accuracy of Tempora (as Tran et al. show in their paper) falls below that of methods they benchmarked.

Additionally, Tempora does not automatically detect cell fates and their lineage pathways or offer single-cell level ordering of cells, all required for the unsupervised plotting of gene trends along detected lineages. This again makes it difficult to effectively benchmark, particularly for real data.
We do acknowledge that in the case of time series data, it is useful to incorporate the sampling time labels and is a feature we would consider adding to VIA in future releases. Such a feature would resemble FlowMAP which uses the adjacency of temporal annotations to determine the graph-edge connectivity.

We therefore consider the set of chosen methods for benchmarking - now including STREAM - to be a fair representation of 'state-of-the-art' methods. We show below (**R3.Q1**) the performance of STREAM on the synthetic datasets and refer to our other dataset specific figures in the main text and gene-trend plots (**Supplementary Fig. S9, S11, S15**) for comparison on real data. We have also added a note in the revised main text and method section highlighting the general rule-of-thumb for choosing methods for benchmarking:

"....lazy-teleporting random walks allow VIA to consistently identify pertinent lineages that remain elusive or even lost in other top-performing and popular TI algorithms we benchmark (Saelens et al., 2019), which are chosen for comparative analysis conditional on meeting several of the following criteria: automated lineage path and cell fate prediction, recovery of complex topologies not limited to trees, scalability and generalizability to multiple single-cell-modalities."

In the Methods section:
"The methods were chosen based on their superior performance in a recent large-scale benchmarking study [4] , including a select few recent methods claiming to supersede those in the study. Specifically, recent and popular methods exhibiting reasonable scalability, and automated cell fate prediction in multi-lineage trajectories, not limited to tree-topologies, were favoured as candidates for benchmarking (See ***Supplementary Table S1*** *for the key characteristics of methods). Performance stress-tests in terms of lineage detection of each biological dataset, automated gene trend prediction along lineages, and pseudotime correlation were conducted over a range of key input parameters ... Methods that focus exclusively on a single data modality or on topology without predicting cell fates and their lineage pathways (e.g. Tinga, Tempora) were generally not included in the benchmarking as they would require manual selection of cell fates and differentiation pathways."*

R2.Q2. An example is given of the analysis of the cell cycle progress of cells using Imaging Flow Cytometry. However this type of analysis has been carried out previously [Blasi et.al. 2016, Eulenburg 2017 - Nat Comms]. The trajectory is not very complex so a simple diffusion map approach can work.

R2.A2. We thank the reviewer for drawing our attention to two very interesting papers using imaging flow cytometry to analyse the cell cycle process. Blasi et al. showcased the ability of trained machine learning algorithms to successfully predict cell stages based on extracted biophysical features. Similarly, Eulenburg et al. also focused on a CNN trained by labeled cell cycle stages and then subsequently used the last layer of the CNN as the input to a t-SNE visualization of the cell cycle progression trend. While they represent valuable findings, we believe that VIA offers a different use case where the labels of cells are not known in advance for graph construction, temporal ordering and the subsequent feature trend analysis. The inclusion of label-free biophysical phenotypes that were absent in the above two studies (i.e. single-cell mass-density and its subcellular spatial distribution), combined with the application of VIA on FACED imaging flow cytometry demonstrates the new significance of combining label-free single-cell biophysical profiles with advanced TI methods (VIA in this case) .

Whilst the trajectory of the FACED image based cell cycle is not complex, we have now added the new **Fig. S23** (also below) to illustrate that Palantir and 'PAGA+DPT', two methods which use Diffusion Maps do not provide a clear interpretation of the linear progression shown by the cells. For instance, PAGA forms S-shaped loops and edges which distort inference of the cell-cycle-related morphology. Palantir is highly sensitive to the choice of root cell as the diffusion map representation disperses G1 cells along the entire trajectory which means that Palantir often finds multiple 'terminal' states which are in fact G1 stages. Also, we note that STREAM places S-phase cells in a separate branch indicating a bifurcating structure. Moreover, VIA is the only method which shows the slow-down of the cell growth during S-phase.

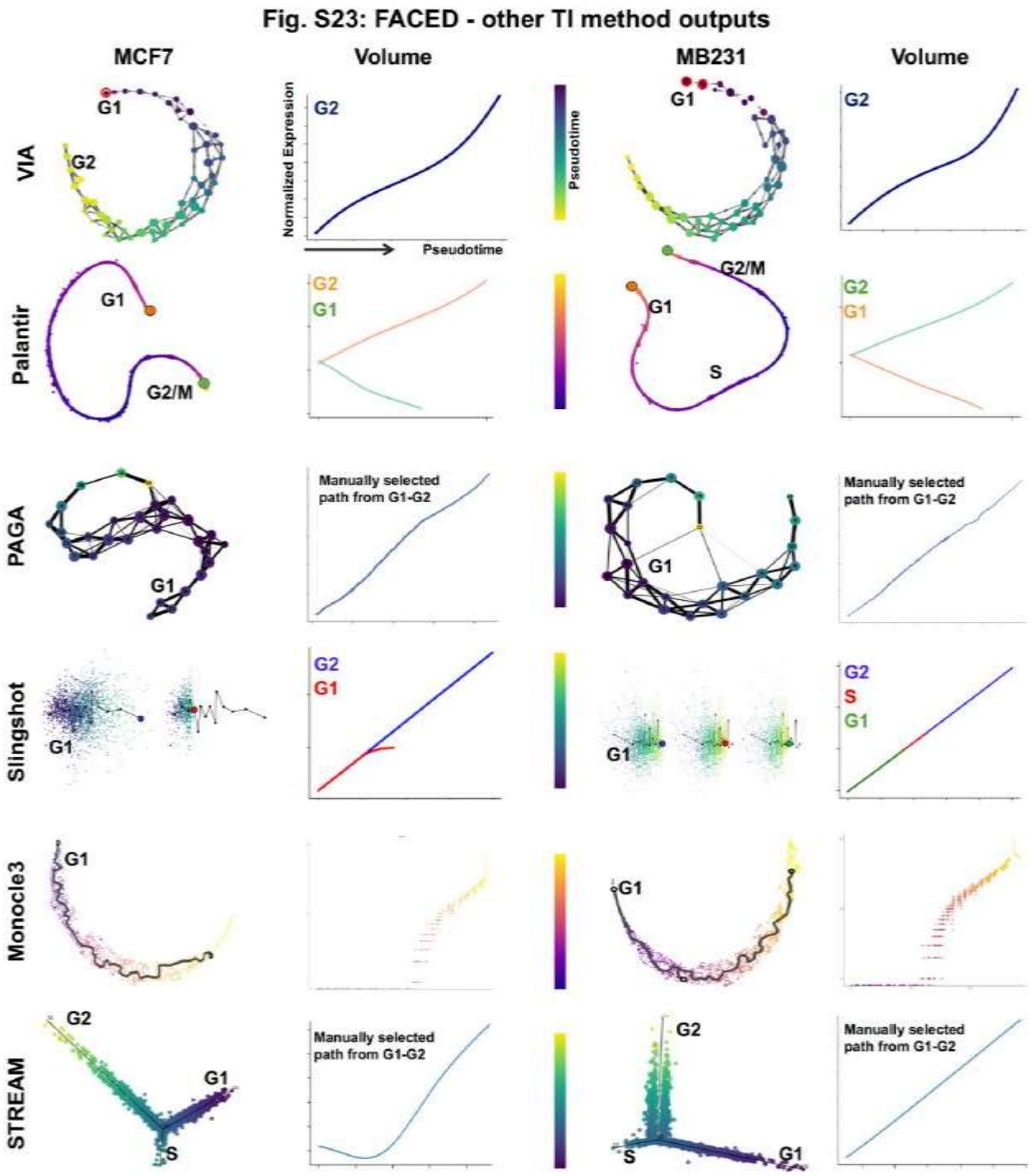

421 ***Fig. S23 FACED biophysical profiles of cell-cycles analyzed by other methods.*** *The topologies and the temporal* *422* *trend of volume inferred by other methods is shown for MCF7 and MDA-MB231. Note that for PAGA and STREAM* *423* *we manually select the branches or clusters used in the trend plots. In STREAM the S cells are placed in a separate* *424* *branch in a bifurcating structure. PAGA structure has an "S-shape" which we do not follow when selecting suitable* *425* *clusters from G1 to G2 state. Many methods such as Slingshot and Palantir show multiple lineages ending at different* *426* *stages along the cell cycle even though the root cell is selected as a G1 stage at the 'tail end' of the data* *427* *representation.*

R2.Q3. The authors also use an ergodic approach (Kafri et.al.2013 Nature) to infer details about certain cell characteristics, however as Kafri discussed, care must be take to not use any predictor measure corrected to the response variable i.e. if you are inferring dry mass, volume then no correlated variables (e.g. cell radius, area etc) should be used in the pseudo time alignment.

R2.A3. We thank the reviewer for this query. Taking the reviewer's suggestion, we probed the features by removing volume and all features highly correlated with volume. Only features satisfying an absolute correlation with volume below 80% (excluding features such as cell dry mass, area, volume) were used to uncover the same size-related trends. The new results are presented in **Fig. S25-S26** .

Running VIA without the cell volume (and volume-correlated) features, we see that VIA still correctly uncover a clear cell-cycle progression and only identifies G2 stage cells as cell fates. It also recovers the slow down in growth during the S-phase. The results are consistent across the two different cell lines (i.e. the MCF7 and MB231 datasets). We also compare the results to PAGA and Palantir (which use diffusion components) to show that relying on the diffusion component space to infer the trajectory does not necessarily offer satisfactory results. For instance, Palantir identifies multiple intermediate cells as final cell fates even though we have carefully provided Palantir with a starting cell at a tail end of its data representation. The graph topology of PAGA, on the other hand, suffers from spurious edges that could confound intuitive interpretation and analysis of TI (e.g. **Fig. S23, S25-S26**).

We would also like to clarify that in our original analysis, the volume (like any other feature) serves to guide the temporal ordering of the cells, and is not used to predict the actual values of other features. The inferred temporal ordering is then used to plot feature expression, thereby allowing us to visualize the changes in expression according to the inferred chronology. We find this to be the standard approach taken by other methods on other omics datasets where marker-gene trends are plotted even though the same gene (or highly correlated ones) were used in the TI.

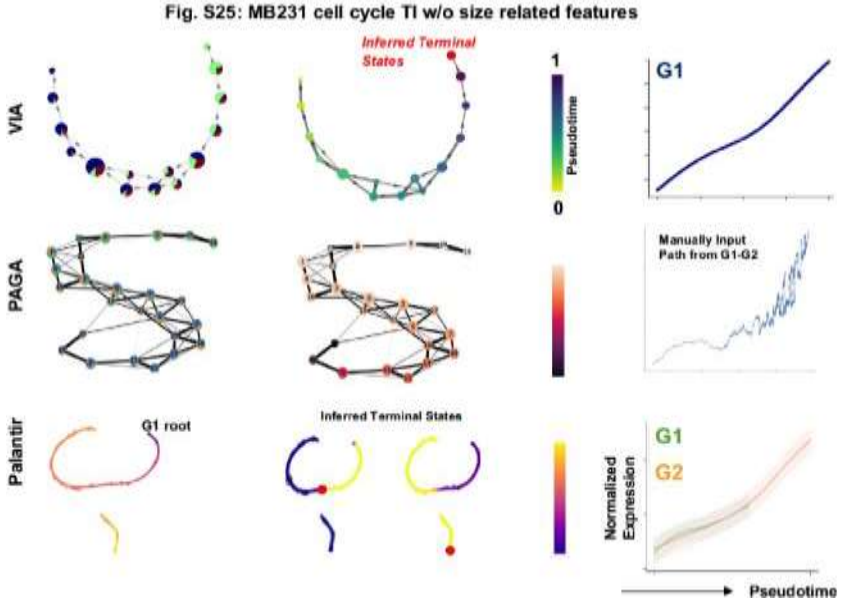

Fig. S25 Cell-cycle TI predicted without cell volume (and volume-correlated) features (MDA-MB231 cells). *Volume and features with $|Corr(x, volume)| > 0.8$ are removed from the input to trajectory inference. We then plot volume along the inferred cell ordering to see whether we detect the correct trend, including the slow-down in S-phase. Note that for PAGA, the clusters from a root cell to a final "G2 cluster" are manually provided.*

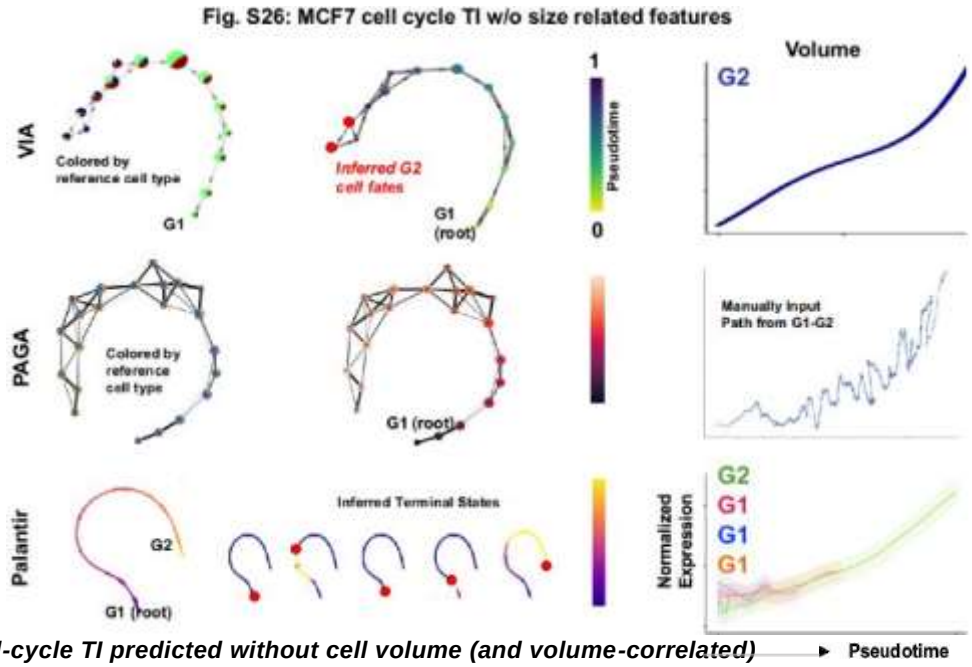

Fig. S26 Cell-cycle TI predicted without cell volume (and volume-correlated) features (MCF7 cells). *Volume and features with an absolute correlation with volume above 80%, i.e. $|Corr(feature, volume)| > 0.8$, are removed from the input to TI. We then plot volume to see if the correct trend along the inferred cell ordering is observed, including a slow-down in S-phase. Note that for PAGA, the clusters from a root cell to a final "G2 cluster" are manually provided.*

R2.Q4. I believe the manuscript is probably better suited to a method type journal as it appears to be an addition to an already large set of algorithms to do this job and also details of some of the examples need to be further elucidated as discussed above.

R2.A4. While we acknowledge that trajectory inference is a rapidly developing field, pushing the limits of current methods in terms of the scalability along feature and sample size, and the generalizability to various topologies has neither been obvious nor straightforward (as discussed in our introduction and evident in the results presented in this work). In this manuscript, we present VIA as a new TI method, using the new strategy of lazy teleporting random walks, to demonstrate its power in many challenging single-cell TI applications (particularly discovering elusive lineages and rare cell fates) across different omics datasets, including the emergent biophysical (imaging) cytometry .

Furthermore, many TI methods tackle either topology (e.g. PAGA, Tempora, TinGa), or the single-cell level ordering and lineage trends without a topological abstraction (e.g. Palantir, Slingshot). In contrast, VIA provides an analysis that can integrate the topology with single-cell level ordering and lineage prediction to allow biologists to perform a more multifaceted analysis. Another key practical consideration is that the speed of VIA allows users to experiment with different parameters and pre-processing methods as multiple runs are inexpensive.

Overall, VIA represents an important technical advancement as well as a unique facilitator for new discovery by allowing biologists to design and explore multi-modal, large-scale experiments. We note that the broad interest in these key strengths is evidenced by VIA's altmetric score of 46 on BiorXiv (top 5% of research) . We believe the advances presented here are sufficiently impactful in the ever-growing single-cell omics community.

REVIEWER #3 (Expertise: trajectory inference using single cell data):

R3.Q1. This paper presents the VIA method for inferring trajectories in single-cell data, regardless of the –omics type. It relies on one metric, the F1-score (that assesses how accurately cell fates were identified by each method), to assess the accuracy of the VIA method and compare it to 5 state-of-the-art methods. This F1-score seems too weak of a metric to me, as it doesn't capture the structure of the returned trajectory. I can think of different trajectories (successively bifurcating, trifurcating, or even disconnected), that could have exactly the same cell fates, and thus return the same F1-score. I would thus recommend adding a second metric, next to the F1-score, that would capture the topology of the different trajectories. Moreover, the F1-score metric that was chosen by the authors doesn't allow them to compare all the tools that they included in the study (as PAGA doesn't automatically detect terminal states). If the paper chose to use only one metric to compare all methods, this metric should at least allow to compare all methods. In my opinion, the paper would benefit from adding at least one more metric to compare the methods on.

R3.A1. We thank the reviewer for the suggestion to add another metric and more directly evaluate accuracy in terms of the topology of the inferred trajectory. We agree that this would provide a more holistic platform to benchmark methods, and also allow for methods which do not predict lineages, like PAGA, to be evaluated. In the revised manuscript, we have therefore revamped the benchmarking analysis of both synthetic and real data in the following ways:

Synthetic datasets: Leveraging the availability of reference models of the topologies and sampling times given by the synthetic datasets, we took a comprehensive quantitative approach using a new set of metrics to systematically evaluate the performance of each benchmarked method.

Real biological datasets: We deepened the gene-trend analysis along the inferred lineages to offer both a quantitative and qualitative comparison across all relevant lineages for each method across 3 datasets which have multiple cell fates of varying population sizes, with known marker genes.

For the synthetic data we 1) defined a new set of metrics (detailed below) that assess multiple layers of the inferred trajectory, including the topology, pseudotime and predicted cell fates and 2) added more synthetic datasets to have two of each type of trajectory (multifurcating, cyclic, connected and disconnected). (**See the new Fig. 2** for an overall summary and **new Fig. S2-5** for a breakdown of the composite metric's components for each topology).

We have also added the description of these new metrics in the main text accompanying **Fig. 2** , and in the method section. Here below is summary in main text:

*"The availability of a reference truth model for the synthetics datasets allows us to quantify TI accuracy using a composite metric which assesses multiple layers of the inferred trajectory including topology, pseudotime and lineage prediction. The metric measures "local" graph similarity between the inferred and reference graphs using the Graph Edit Distance (GED), an F1-Branch score (which labels branches as True or False Positives, or the lack thereof as a False Negative), and the "global" graph similarity is computed using the Ipsen-Mikhailov measure (**Methods**). The breakdown of the composite score is shown for each dataset in **Fig. S2-S5** .*

The differences in accuracy between VIA and other methods is most notable in complex topologies, particularly those with disconnected components comprising various connected topologies."

Further details of the composite accuracy score as well as the figure showing the individual components of the score for each topology are now available in the new **Supplementary Note S3** :

"We use 9 synthetic datasets to benchmark the performance of VIA and other methods on a variety of trajectories and topologies ***(see Fig. 2)*** *. The 9 synthetic datasets are generated using DynToy and contain 1000-3000 cells across 1000 features. They span (bi/multi) furcations, cyclic, connected (which are combinations of cyclic and furcating) and disconnected (which are combinations of all the aforementioned). The composite accuracy metric assesses multiple layers of the inferred trajectory, taking into account the topological similarity between the reference model and the inferred topology, the correlation between the real and 'pseudo' times, as the prediction accuracy of the terminal cell fates (lineages). For certain metrics, the absolute measurements of similarities or differences are converted into a percentage scale such that 100% corresponds to the highest score. The composite metric is the arithmetic mean of the 5 scaled metrics.*

Ipsen-Mikhailov (IM) *: IM distance is used to measure the similarity of global graph topology. The IM ranges from 0 to 1 and equals the difference in spectral densities of two graphs. $IM(G_1, G_2) = 0$ implies that the graphs are isospectral. Unlike the Graph Edit Distance and the F1-branch score, where only the structure of each link's immediate neighbourhood contributes to the distance value, the IM considers the structure of the whole topology. We use $1 - IM$ for the composite accuracy score.*

$$IM(G_{TI}, G_{REF}) = \sqrt{\int_0^{\infty} [\rho_{REF}(\omega) - \rho_{TI}(\omega)]^2 d\omega} \qquad [19]$$

$$\rho(\omega) = \sum_{k=1}^{N-1} \frac{\gamma}{(\omega - \omega_k)^2 + \gamma^2} \qquad [20]$$

$\rho(\omega)$ is the graph spectral density as a sum of Lorentz distributions, ω_k are the vibrational frequencies given by $\sqrt{\lambda_i}$ where λ_i are the eigenvalues of the Graph Laplacian. γ is the half width at half maximum.

Graph Edit Distance (GED) *: is defined as the cost of converting G_{TI} to G_{REF} with the least possible number of operations. Each operation has a cost of one and includes insertion/deletion of edges and nodes. Oftentimes graph edit distances like the (e.g. GED, Hamming distance) are normalized by the entire set of possible edges $N(N-1)$, but this creates an inflated sense of accuracy in the case of very sparse graphs like the reference topologies of the synthetic datasets. We therefore normalize by the sum of nodes and edges in G_{REF} . 1- 'Normalized' GED is used in the composite accuracy measure.*

F1-Branch score: *is applied to the local branch accuracy and defined as follows . A False Negative edge in the inferred model is when there is an edge in the reference model connecting clusters/cell types/groups that is absent in the inferred trajectory. A False Positive edge in the inferred model is when an edge occurs in the inferred model that is not actually present in the reference model. A True Positive Edge is one that exists in the inferred model that also exists in the reference. These three measurements are used to compute the F1-score.*

$$F_1 = \frac{tp}{tp + 0.5(fp+fn)} \qquad [21]$$

Temporal Correlation: *Given the sampling times of the synthetic data, we use the Pearson Correlation coefficient as a measure of how closely the inferred pseudotime follows the true sampling times. σ_X is the standard deviation of X, and μ_X is the mean.*

$$\rho_{x,y} \stackrel{E[(X-\mu_X)-(Y-\mu_Y)]}{=} \frac{}{\sigma_X \sigma_Y} \qquad [22]$$

F1-Cell Fate score: *We use the harmonic mean of recall and precision as given by Eq.[21] to quantify the prediction accuracy of terminal states. tp is a true-positive: the identification of a terminal cluster that is in fact a final differentiated cell fate; fp is a false positive identification of a cluster as terminal when in fact it represents an intermediate state; and fn is a false negative where a known cell fate fails to be identified."*

Fig. 2: VIA performance comparison for complex hybrid topologies

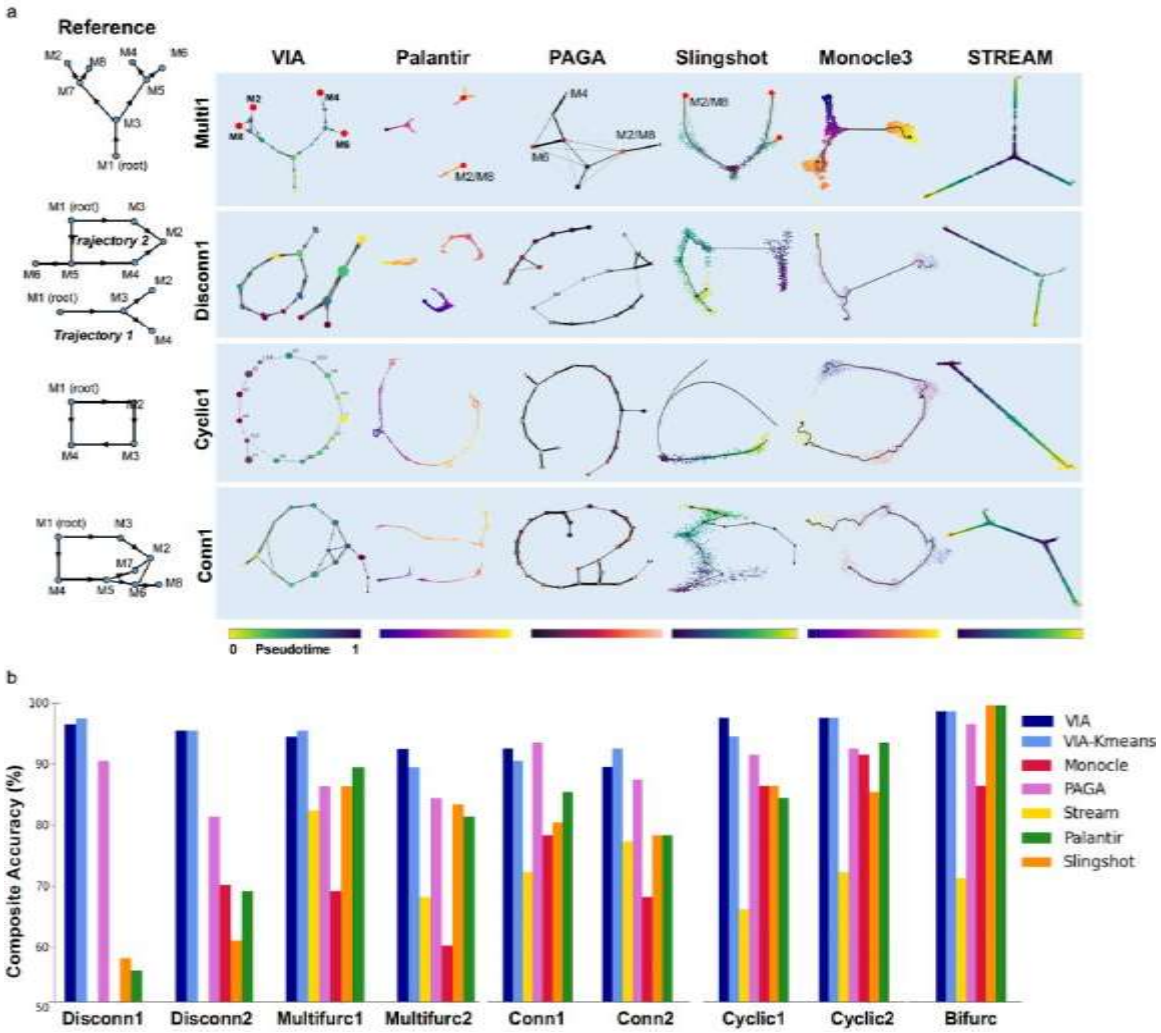

Figure 2 TI performance comparisons on complex hybrid topologies. (a) *Topologies of four representative synthetic datasets (Multifurc1, Cyclic1, Disconn1 and Conn1) output by different TI methods. The reference topologies are shown on the left. Each dataset contains 1000 'cells' and is run with 10 principal components and KNN = 20. VIA is shown at the cluster graph level but can also be projected to the single-cell level as shown in later examples.* ***(b)*** *Composite accuracy score is shown for each method across all 9 synthetic datasets (detailed breakdown available in* ***Supplementary Fig. S2-S5*** *). Note STREAM does not work on the Disconnected data (producing highly distorted results) and therefore excluded for assessment in Disconn1 and Disconn2.*

Quantitatively evaluating the real datasets beyond lineage detection is more challenging. We approached this by deepening the gene-trend analysis and comparing the unsupervised gene-trends inferred by VIA to the lineage gene-trends predicted by other methods. This is explained in the revised **Methods** as follows:

"Downstream analysis enabled by the automated lineage prediction capabilities of each method is key to facilitating the exploration of biological data. The unsupervised gene-trend analysis inferred by VIA is compared to the lineage gene-trends predicted by other methods both quantitatively and qualitatively. We follow an approach used by Chen et al. [63], where pseudotime is correlated against expression of a marker gene known to monotonically increase along the lineage. The gene-expression of such markers can be considered a surrogate for the correct sampling time and thus the resulting correlation is an indication of the accuracy of cell ordering by pseudotime. We also provide a side-by-side comparison of the predicted topology and gene-trends generated by each method to visually assess how well separated the predicted lineages are (e.g. if multiple lineages that represent distinct cell fates exhibit significant cross-talk in the plotted trends or uniquely express the genes most relevant to their lineages). The Pearson correlation coefficient is given by $\rho_{x,y}$, where σ_X is the standard deviation and is the mean of X μ_X

$$\rho_{x,y} = \frac{E[(X-\mu_X)-(Y-\mu_Y)]}{\sigma_X \sigma_Y}$$

Built-in functions for gene-trend plotting (wherever available), and in other cases manually selection of branches/clusters or extension of a method by adding GAMs to general gene-trend curves are required to facilitate comparison (e.g. PAGA and STREAM). Additionally, when methods cannot automatically detect all the relevant lineages, we either chose the most relevant lineage (e.g. for the megakaryocyte lineage, we plotted its CD41 marker gene along the detected erythroid lineage which often absorbed the smaller megakaryocytic line), or we noted that the lineage was missed (e.g. in the endocrine dataset the delta cells were often missed) when the lost lineage was not an obvious part of another lineage. Given that these nuances are not necessarily captured by the correlation coefficient, the outputs of the gene-trend plots inferred by each method are shown for three datasets which have multiple lineages of different abundances, and well known lineage markers (scRNA-seq and scATAC-seq hematopoiesis, and endocrine genesis in ***Supplementary Fig. S9, S11 and S15*** *)."*

For Slingshot, Palantir and VIA, the comparison is fairly straightforward as these methods offer single-cell level temporal ordering as well as lineage likelihoods which can be used to infer the trends of genes. PAGA however requires manual selection and ordering of a pathway from root to desired cell fate before plotting the gene trend in relation to pseudotime by using a sliding window approach. For STREAM we again selected only the desired branching pathway for a given lineage to minimize potential cross-talk. The lack of single-cell level differentiation pathways in STREAM (where we could only select pathways at the branch level), lowers the quality of the plotted trends. We then applied GAMs in order to smooth the gene trends so that the computed correlations could be compared to the other methods. Monocle3 is more challenging as its gene-pseudotime function does not consider lineage pathways but rather orders all cells along the inferred pseudotime before fitting a curve. This oftentimes resulted in the curve fitting being so noisy it overwhelms the original data.

Here, we briefly highlight key features in the gene trend comparison for each of the three real datasets:

scRNA-seq hematopoiesis (Fig. S9): The dataset contains two types of dendritic cells (the classical and the plasmacytoid DCs). We point out however, that for most methods only a single lineage is upregulated for the Dendritic marker IRF8. Similarly, the CD41 (ITGA2B) is often upregulated by the erythroid lineage rather than by a distinct lineage exclusive to the megakaryocytes (e.g. Slingshot's 'blue' curve is the only lineage showing both CD41 and GATA1). In PAGA we note that the pseudotime scale is distorted due to the weak linkage to the CLP (B cells) lineage and the gene plots are very noisy. Monocle3 also separates the CLP lineage away from its progenitors which means it cannot be reached from the HSC state. For other values of KNN/PCs, Monocle3 often even splits the erythroid lineage as a disconnected group from the progenitors. STREAM sometimes places the same cell type along multiple distinct branches which results in the additional up/down regulations seen in the predicted gene curves.

scATAC-seq hematopoiesis (Fig. S11): Monocle3 splits the monocyte and CLP lineage away from the intermediate states, making them undetectable from the HSCs. For Slingshot, we find that the F1-cell fate scores are generally quite poor, not because it fails to detect the relevant lineages, but because it detects several intermediate stages as terminal cell fates. However, when plotting the gene trends we select only the 4 that most distinctly capture the relevant cell fate lineages. Although the marker genes are significantly upregulated for the selected lineages, we see that often the correlation scores are low because the lineage pathways include cells that are irrelevant to the terminal cell fate and cause the expression levels to drop at later stages along the branch. The visualization of Slingshot's topology (shown in the rightmost column of **Fig. S11**) when using more than a few PCs is also difficult to interpret because the principal curves are made on the PCA input, but cannot be linked to a t-SNE/UMAP visualization. It thus resorts to plotting the lineage curves on the first two PCs. The coarse branching structure of STREAM (even though the full pipeline for complex datasets is followed) again means that cells that are not very relevant to a certain lineage are included in the branches, thus contributing to that cell fate and perturbing the gene trends even when using the same cubic spline function as applied in VIA. As seen in the branching structure of the VIA graph, the granularity of the VIA's branching structure allows for the computed lineage-probabilities to more accurately reflect the likelihood of cells leading to a particular cell fate, and consequently refine the plotted gene trends.

scRNA-seq endocrine genesis (Fig. S15): VIA, Slingshot and STREAM perform well on the endocrine dataset, consistently identifying the 4 pancreatic islets. The gene trends however are superior for Slingshot and VIA where lineages exhibit less intermingling along a determined single-cell differentiation pathway, resulting in clearer gene expression of the lineage specific markers. VIA can distinguish between the two Beta cell types (based on the difference in Ins1 and Ins2) even though the underlying number of clusters is similar (PARC automatically identifies ~15 clusters, and Kmeans used by Slingshot is set to 15).

The correlation coefficients for cell ordering along lineage marker expression are summarized in the new subfigures in **Fig.3-4:**

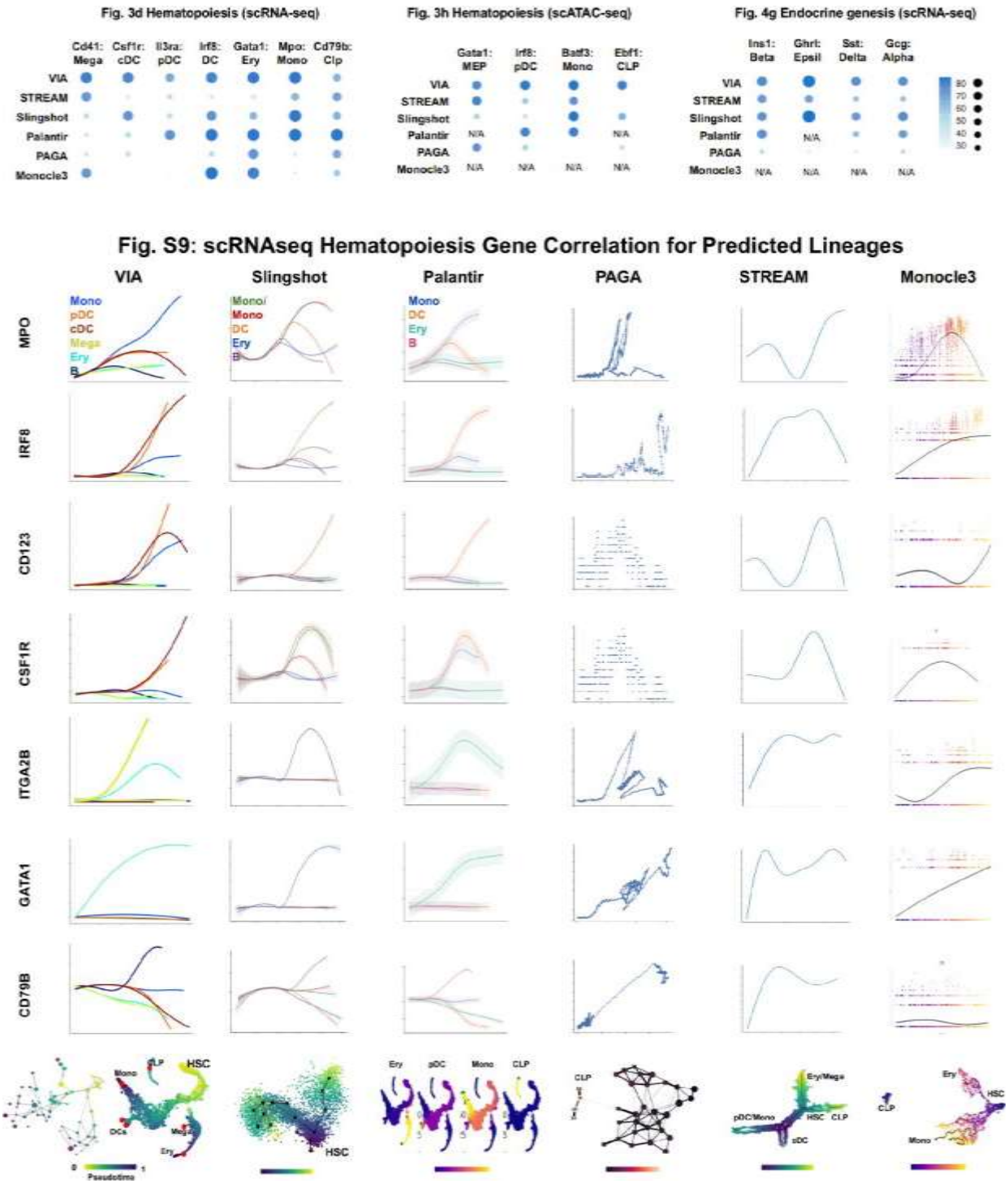

644 ***Fig. S9 Comparison of marker gene correlation computed by different TI methods (for predicted lineages in***
645 ***scRNA-seq hematopoiesis).*** *Automated gene expression plots as a function of pseudotime for the lineages*
646 *associated with 6 specialized cell types. For PAGA and STREAM we manually select the order of clusters/branches*
647 *towards a terminal state. PAGA uses a sliding window approach to compute the expressions based on the selected*
648 *clusters, whilst for STREAM we apply GAMs to plot the expression. For Slingshot's topology, the black lineage curves*
649 *cannot be aligned with the t-SNE embedding, but we show the colored temporal ordering of cells on the t-SNE for*
650 *ease of comparison to other methods.*

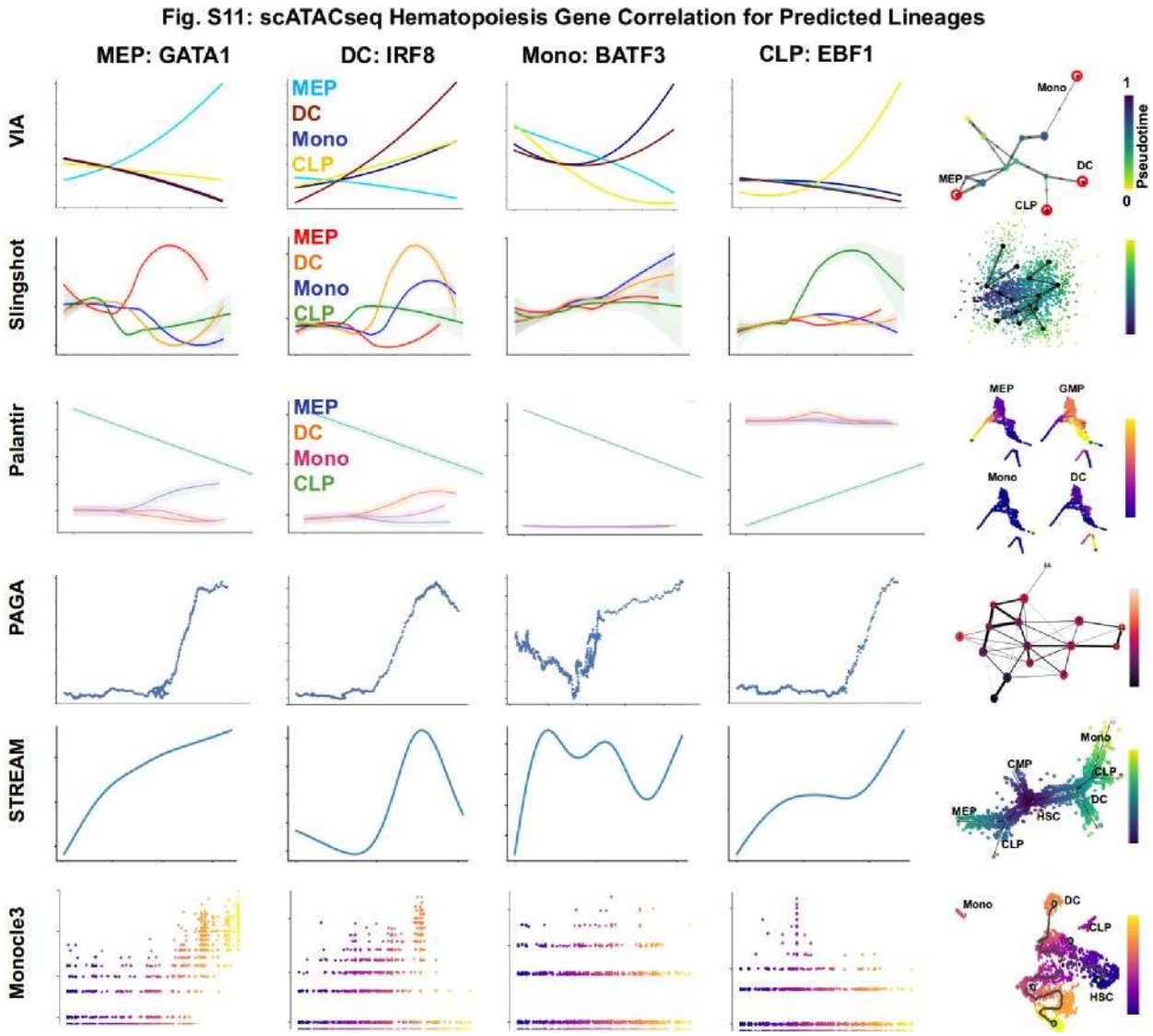

Fig. S11 Comparison of marker gene correlation computed by different TI methods (for predicted lineages in scATAC-seq hematopoiesis). *Automated gene expression plots as a function of pseudotime for the lineages associated with CLP, MEP, Monocyte and DC committed cells. For PAGA and STREAM we manually select the order of clusters/branches towards a terminal state. PAGA uses a sliding window approach to compute the expressions based on the selected clusters, whilst for STREAM we apply GAMs to plot the expressions. Monocle3 did not plot fitting curves on this dataset.*

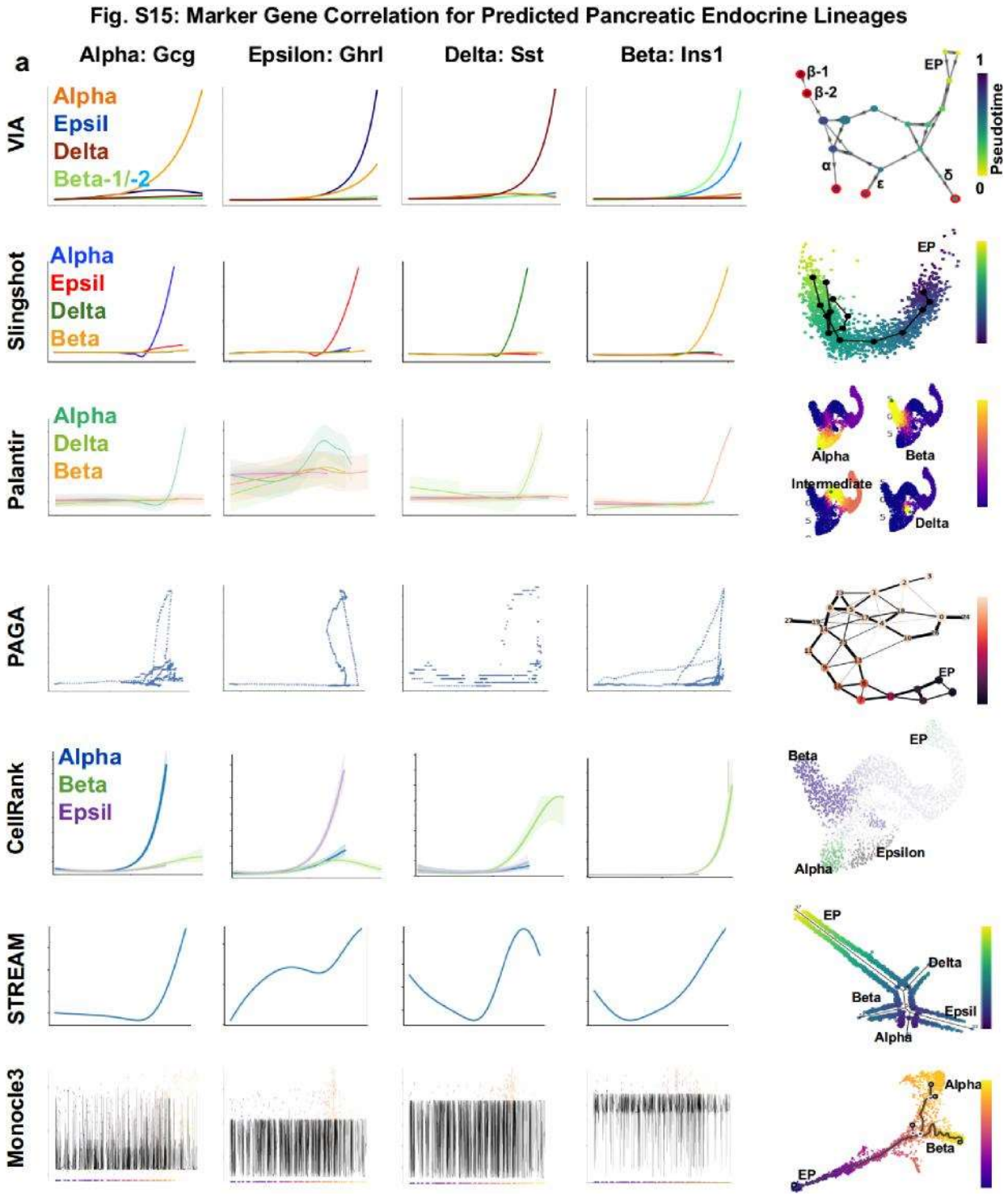

Fig. S15 Comparison of marker gene correlation computed by different TI methods (for predicted endocrine lineages). *Automated gene expression plots as a function of pseudotime for each of the 4 pancreatic islets: Alpha (Gcg), Beta (Ins1 and Ins2), Delta (Sst) and Epsilon (Ghrl). For PAGA and STREAM we manually select the order of clusters/branches towards a terminal state. PAGA uses a sliding window approach to compute the expressions based on the selected clusters, whilst for STREAM we apply GAMs to plot the expressions. The dark curves on the Monocle plots are very noisy and overwhelm the original data points.*

R3.Q2. Small comment related to the previous one: in figure 2a), the authors state that the F1-score can't be computed for PAGA as this method doesn't automatically return cell fates. However, an F1-score was then computed for PAGA for the cyclic dataset (presented figure 2b), and disconnected dataset (presented in figure 2c). Please clarify in the text, in the methods, or in the description of figure 2 how and why the F1-score was computed for some datasets but not for others. The fact that the F1-scores presented on the right of figure 2 correspond to a different set of methods for each dataset is confusing.

R3.A2. We apologize for the confusion and we have changed the figure such that it is now more easily interpretable. In the previous version of the figure, the F1-scores for the cyclic and disconnected trajectories were F1-branch (graph-edge) scores, not F1-cell fates scores - and quantified the graph edge topology similarity between the reference and inferred topologies. We were therefore able to include PAGA for this particular graph-similarity accuracy measure.

R3.Q3. It is unclear to me why, in each figure where VIA is compared to other methods, it is not being compared to all the other methods. For example, why did the authors choose not to include the results of PAGA in figure 4? Of Monocle3 in figure 7?

R3.A3. As detailed in our response above (**R3.A2**), we have extended our comparisons for each dataset to include all methods (including now PAGA for gene trends in **Fig. 4** and Monocle3 in **Fig. 7**). In the case of PAGA, we generally do not perform extensive stress-testing across PCs/KNNs in most datasets as PAGA cannot predict cell fates. We have however included PAGA in our comparison of gene-correlation comparisons where we were able to manually select the pathway from root to a manually selected appropriate cell fate cluster. PAGA is also part of the synthetic dataset analysis where the composite score for PAGA is calculated by excluding the F1-cell-fate score and including the other 4 metrics. For the MOCA dataset in **Fig. 6** , we include PAGA in the comparisons because we do not quantitatively assess the performance as there is no clear reference truth. Therefore we can visually compare and contrast the topologies inferred by VIA, PAGA and Monocle3 (based on the UMAP input) for various KNN and PCs as these approaches can be reconfigured and run in a reasonable timeframe. Since there is no clear reference topology and we need to rely on the sampling times and annotated cell types to understand this dataset, we have provided an extensive discussion on the inferred branching structure in both the main text as well as in **Supplementary Note S3** .

R3.Q4. The paragraph starting at line 378 should, in my opinion, be rephrased. Historically, the first trajectory inference (TI) tools were designed to be applied on cytometry data (Wanderlust, Monocle). This type of data contains a much better ratio of cells over features than scRNA-seq data, and suffers less from sparsity, which typically makes it easier to find trajectories in this type of data. However, the way the paragraph is written now, the authors seem to suggest that most TI methods can only handle transcriptomic data, and that handling cytometry data would be a new advantage of VIA. I would thus advise to rephrase this paragraph to avoid misleading the reader.

R3.A4. We thank the Reviewer's suggestion for further articulating the argument/rationale of the cytometry application of VIA. Our intention is to convey that many methods are frequently only tested on a single experimental modality, even if they can in theory be extended to other types of datasets. We

merely wish to point out that we test VIA for practical compatibility to a diverse range of omic datasets. We have revised this paragraph accordingly as follows,

" Broad applicability of TI beyond transcriptomic analysis is increasingly critical, but existing methods have limitations contending with the disparity in the data structure (e.g. sparsity and dimensionality) across a variety of single-cell data types. We have thus far shown that VIA can be used to successfully interrogate scATACseq, scRNAseq and their integrated data, and now proceed to further investigate whether VIA can cope with the significant drop in data dimensionality (10-100), as often presented in flow/mass cytometry data, and still delineate continuous biological processes."

R3.Q5. The authors emphasize the fact that VIA doesn't require any user input parameters, compared to other methods. Only when reading the methods section do we discover that VIA needs the user to define a starting point to run. This should be stated earlier in the paper in my opinion (around line 25 for instance), as this is an information that any potential user of the method will be interested in. Side comment: as PARC allows a fast visualisation of the data, I'm wondering if allowing the user to choose a starting point in this representation of the data would be a nice way to simplify the choice of a starting point for the user.

R3.A5. We have revised the text in the Algorithm section of the main text to indicate that VIA requires the user to select the root node cell or cluster:

"The root (starting point) is designated by the user either as a single-cell index or using group or cluster level labels."

We observe that the benchmarked TI methods require either a single cell to be initialized as the root cell (Palantir), or selected by the user as a cluster/milestone after an initial topology is constructed (Monocle3, PAGA, STREAM). Since the initialization of a root by group-level or single-cell annotation depends on the information available, we allow the user to choose either of the two approaches and have added the following explanation in Methods:

"The root cell is initialized by the user in one of two ways: If for instance there are some cell type/group/cluster level labels available in advance, the desired starting group can be indicated to VIA, which will then automatically select a cluster in its cluster-graph that contains a majority of this particular cell type/group classification. In the case of many clusters satisfying this criteria, VIA selects the cluster in the graph that has connectivity metrics indicative of a root (leaf) node (such as low betweenness and low centrality). The user can also choose to provide a specific single cell as the root node. In case the user wishes to select the root based on the VIA graph, one would save the VIA-cluster-graph labels and use them to guide selection of the root as described in the first approach."

R3.Q6. The authors highlight the fact that the VIA method's computational advantage allows it to process larger amounts of dimensions, avoiding information loss due to dimensionality reduction. However, they test VIA on all original genes only in one dataset (presented in figure 4), and apply VIA on PCs for the other datasets. It would be interesting to see how the method performs on the original dimensions and how it compares to other methods on the synthetic datasets, and in figure 3.

R3.A6. We thank the reviewer for enquiring about our approach to 'high dimensional' feature inputs. We first explain the approach taken in our paper for benchmarking and general performance analysis, and then introduce the new analysis we have done to test VIA on gene-count features without any PCA (or other dimensionality reduction). We also invite the reviewer to read our **response (point 2) to the Editor** above where we commented on this substantial addition to the paper.

Discussion and context of original analysis:
In our original analysis of various datasets, we showed that VIA handles a broad range of input feature dimensions that are used to characterize various omic datasets. Imaging and mass cytometry features tend to remain within 10-100 features (antibodies or morphological features) which VIA parses without any dimensionality reduction. On the other hand, scRNA-seq produces 5000-15000 genes even for small sample sizes of hundreds or a few thousand cells and it is common to use a dimensionality reduction such as PCA to enhance the signal in the data and avoid the curse of dimensionality, before running further unsupervised computational analysis. Since all the benchmarked methods require PCA, and afterwards often a second stage of further dimensionality reduction (e.g. UMAP, MLLE, diffusion maps) before performing TI, we found that including PCA in the pre-processing pipeline allowed more consistent comparison across all methods.

Several TI methods, including top-performing ones like Slingshot, STREAM and Monocle3 require or highly recommend further reducing the dimensionality using a second method such as UMAP, TSNE or the like. Other methods like Palantir and PAGA which can receive raw features (e.g. for cytometry data) or a higher number of PCs (in the case of gene data) involve steps under the hood that subset the number of diffusion components (default of 10 eigenvectors and an even lower number of diffusion components in PAGA and Palantir) retained for further TI analysis. **See the new Supplementary Note S5** and **Fig. S27** for more details on the dimensionality steps used by the different methods. We found that forcing other methods to compute directly on the genes by overriding dimensionality reduction and subsetting of components resulted in distorted topologies (**Fig. S27a**).

New analysis on full feature inputs:
However, to stretch the capabilities of VIA, we now show that it can sensibly process both real and synthetic data using several thousands of genes without any form of dimensionality reduction. We used the synthetic ~1000 'cell' datasets spanning various topologies to observe how faithfully VIA uncovers topology, pseudotime and cell fate prediction when using all 1000 features. These features were provided to VIA without any dimensionality reduction and yielded results very consistent with the underlying 'ground truth model' **Supplementary Fig. S27** (distinguishes between "VIA-Full" and VIA-PCA, while all other methods are run using PCA first). We refrain from a full benchmarking against other methods as they are not designed to handle such high dimensionality. For instance, Slingshot and STREAM can take several hours on a few thousand cells when the dimensionality exceeds 100 and Monocle3 will not run without a UMAP embedding. PAGA and Palantir depend on using only a small subset of eigenvectors

and diffusion components, without which they produce unreasonable answers (e.g. PAGA results in a fully connected cluster graph as seen below in **Fig. S27** and Palantir overly fragments the data such that the topology cannot be interpreted visually).We therefore can only reasonably compute the composite accuracy metric for VIA on the full feature sets, and show the TI outputs of PAGA and Palantir when we override any 'under-the-hood' subsetting of features to show that a full comparison would not be feasible.

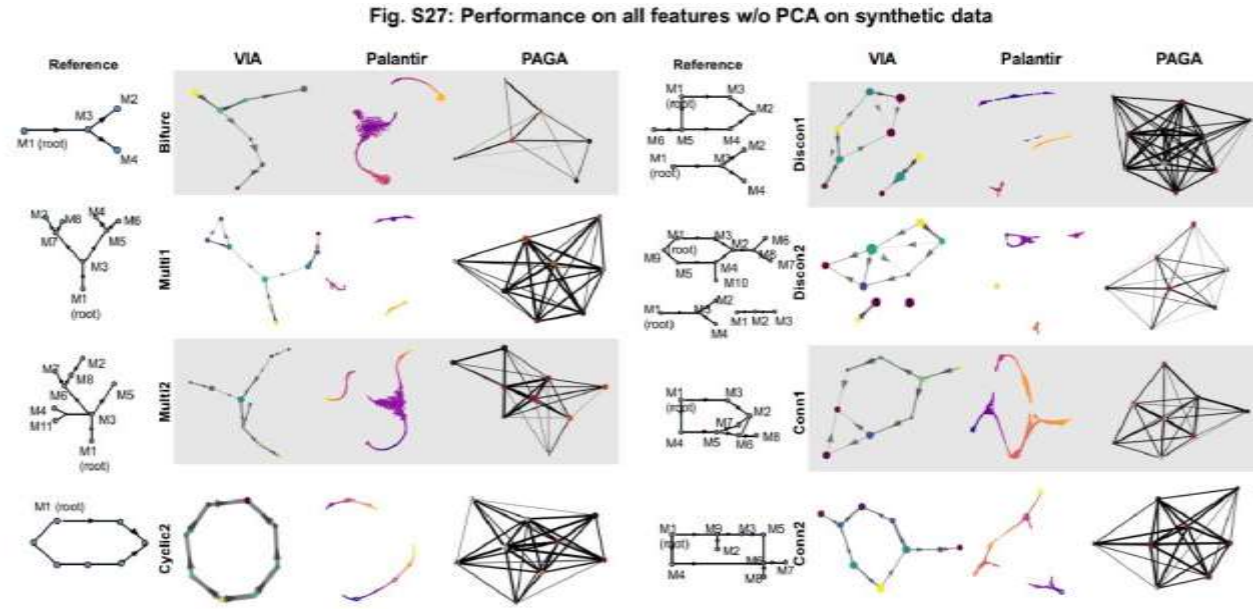

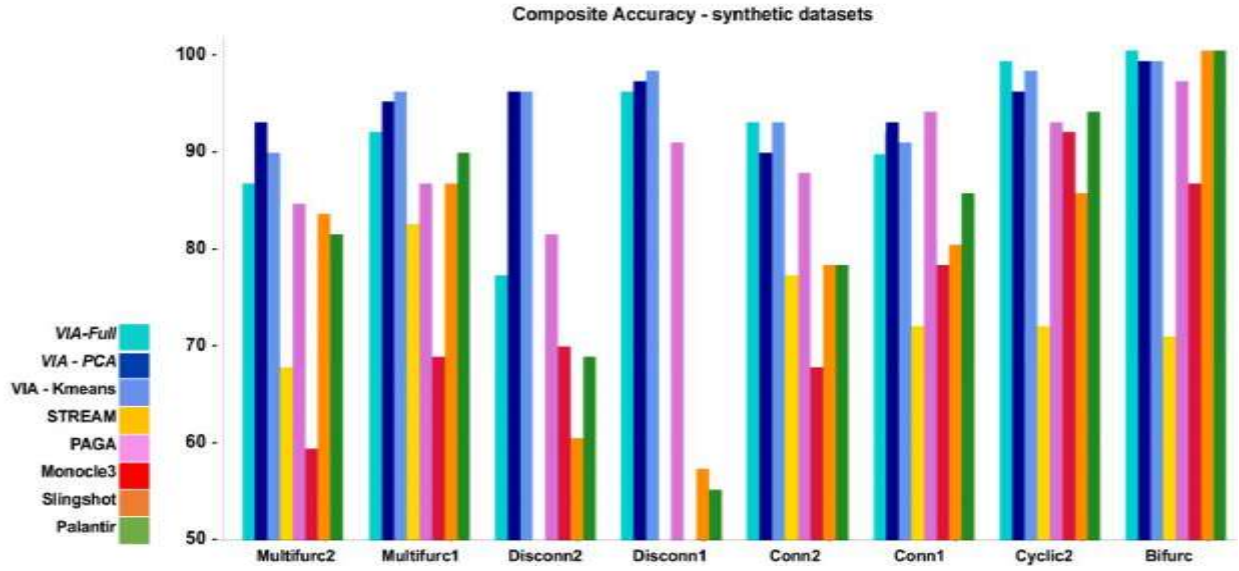

Fig. S27 TI performance comparison with full feature input using synthetic data (no PCA) (a) *Sample outputs of VIA topology when using all 1000 features without PCA compared to PAGA and Palantir. Although the runtimes for PAGA and Palantir are reasonable, their outputs are distorted due to overriding the PCA and subsetting of diffusion components.* ***(b)*** *Composite accuracy scores of VIA when using the full-feature input (VIA-Full), compared to VIA using PCA (VIA-PCA), VIA using Kmeans (and PCA) and all other TI methods which use PCA. We see that VIA can achieve good accuracy even without the PCA step for many of the synthetic datasets.*

R3.Q7. Comment related to the previous one: it is surprising to see that VIA performs optimally when applied on > 6000 HVGs in figure 4, while Slingshot performs best on less than 2000 HVGs (which is more expected). This might be due to the fact that the F1-score captures only the accuracy of the end states recovered by the different methods, and doesn't represent differences in topology. It would be interesting to see whether the same increase in accuracy is observed when using more HVGs in the synthetic data and in figure 3.

R3.A7. We first wish to clarify that the table (in the original **Fig. 4, now Fig. S1c**) indicates the number of HVGs used to compute the PCs before using a range of these PCs as inputs to the different algorithms. In the main text and the purpose of method comparisons, we pre-processed these datasets by following the same protocols as their authors (**See Methods and Supplementary Tables S4-S5**). As mentioned above in **R3.Q6** , other methods do not lend themselves to considering 1000s of features without some form of dimensionality reduction, and thus we limit the assessment of high-feature-inputs on real data to only VIA.

For the purpose of evaluating the topological consistency and cell fate prediction when the input is a range of HVGs without any PCA or other dimension reduction, we examine two real datasets (scRNA-seq endocrine genesis and hematopoiesis) chosen because they are multi-lineage and have cell populations of varying sizes (See new **Fig. S28-S29**). When using the genes as a direct input (after basic filtering and log-normalization), we consider the choice of number of HVGs provided directly to the algorithm as a parameter that could influence the outcome. For both datasets, we visualize the stability in topology across a range of HVGs by showcasing the topological outputs side-by-side. The nodes are colored by pseudotime, with the relevant lineages colored according to the legend.

scRNA-seq hematopoiesis (Fig. S28): In general, the hematopoietic dataset yields high-quality results when using 500-5000 genes (**Fig. S28d**), with three main branches appearing: the CLP (B cells) branch, erythroid/megakaryocytic branch and monocytic/dendritic branch. Within these main branches, the DCs are typically separated (as shown by the colored branches) from the monocytes (evidenced by the unique upregulation of IRF8 in the DC lineage, and not by the monocyte lineage), and the erythroids from the megakaryocytes (the upregulation of CD41 in the lineage associated with megakaryocytes compared to the erythroid lineage). As the number of HVGs exceeds 5000, the structure deteriorates. This is expected given the number of features would begin to significantly exceed the number of datapoints (cells).

scRNA-seq murine endocrine genesis (Fig. S29): Surprisingly, even though the number of cells is only a few thousand, the pancreatic dataset tolerates using up to 10,000 HVGs without sacrificing topology or cell fate prediction. The gene trends are plotted for the automatically predicted 4 lineages (for the 1000 HVG case), and correspond to the 4 pancreatic islets. As shown by the topological outputs, the sustained cell fate identification of the islets is also accompanied by a topology that is biologically consistent. The Ngn- EPs progress towards *Ngn+* , then *Fev+* and then branch towards the more committed lineages. Interestingly we see two groups of *Fev+* populations branching from the *Ngn+* populations which subsequently progress towards the distinct cell lines. This is consistent with an observation by Bastidas-Ponce 2019 who also noted the emergence of two *Fev+* cell types after the *Ngn3+* state.

Fig. S28: VIA on 500HVG of Hematopoiesis

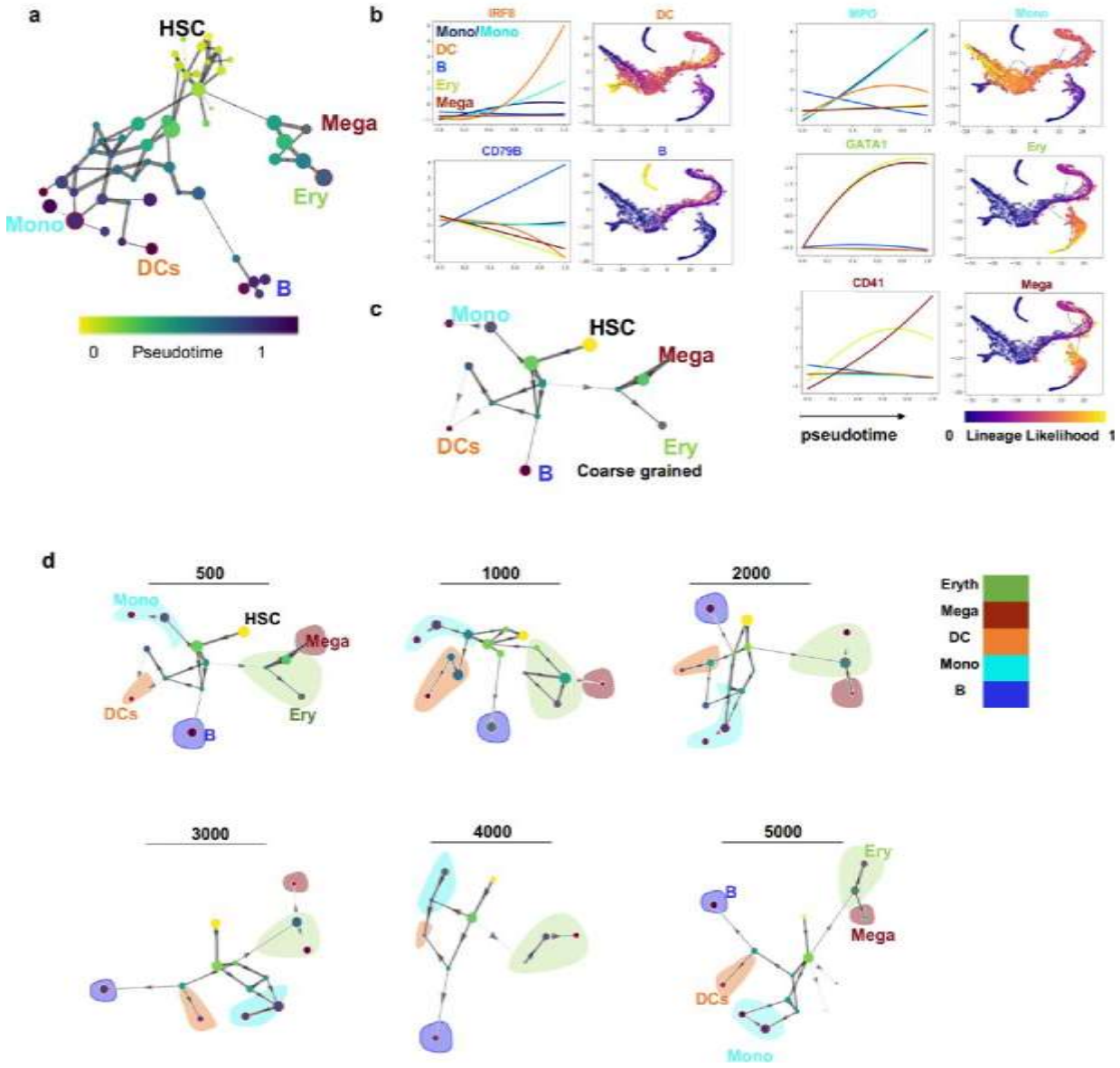

Fig. S28 Highly variable genes (HVGs) as unprocessed input using the scRNA-seq data of hematopoiesis (no PCA) (a) *VIA graph on 500 HVGs without PCA* ***(b)*** *unsupervised plotting of gene trends vs. inferred pseudotimes for predicted lineages.* ***(c)*** *Coarse grained VIA graph.* ***(d)*** *VIA graph topology for increasing number of HVGs without PCA show that the overall pronged topology is stable with erythroid and megakaryocytic branches on one side of the HSCs, and the monocytes and DCs on the other side.*

Fig. S29: VIA on HVG of Endocrine genesis

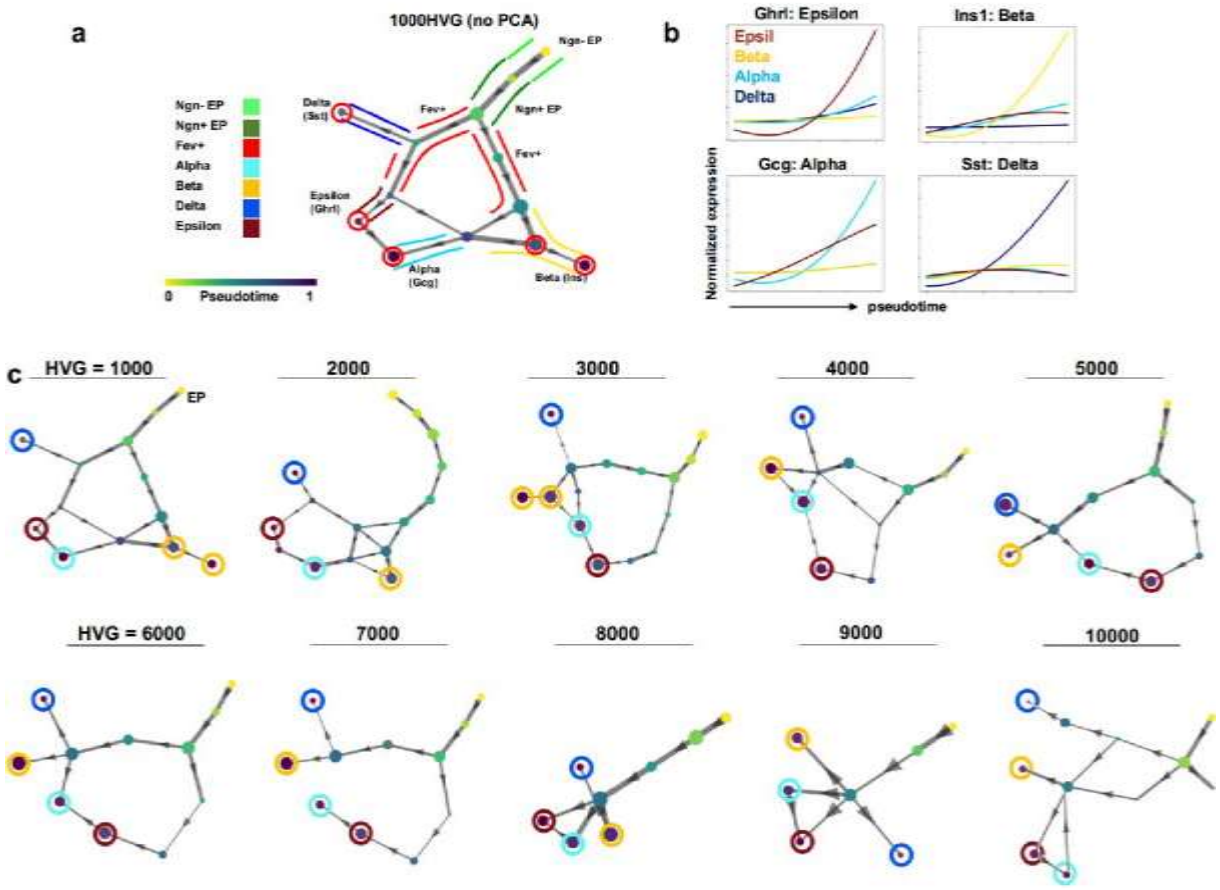

Fig. S29 Highly variable genes (HVGs) as direct input using the scRNA-seq data of endocrine genesis (no PCA) (a) *Overall graph level topology of VIA, nodes colored by inferred pseudotime and automatically detected terminal nodes circled red.* ***(b)*** *Marker gene expression plotted for each lineage shows that each cell fate and pathway uniquely leads to the islet fate associated with that marker gene.* ***(c)*** *Topology of endocrine dataset for different number of HVGs, continues to represent the overall progression from EPs to bifurcation of Fev+ cells that lead to the different islets.*

References

1. Chen, H., Albergante, L., Hsu, J.Y. et al. Single-cell trajectories reconstruction, exploration and mapping of omics data with STREAM. Nat Commun 10, 1903 (2019). https://doi.org/10.1038/s41467-019-09670-4
2. Saelens, W., Cannoodt, R., Todorov, H. et al. A comparison of single-cell trajectory inference methods. Nat Biotechnol 37, 547–554 (2019). https://doi.org/10.1038/s41587-019-0071-9
3. Gerard, D. Data-based RNA-seq simulations by binomial thinning. BMC Bioinformatics 21, 206 (2020). https://doi.org/10.1186/s12859-020-3450-9
4. Stassen SV, Siu DMD, Lee KCM, Ho JWK, So HKH, Tsia KK. PARC: ultrafast and accurate clustering of phenotypic data of millions of single cells. Bioinformatics. 2020 May 1;36(9):2778-2786. doi: 10.1093/bioinformatics/btaa042.
5. Qiu, P. Embracing the dropouts in single-cell RNA-seq analysis. Nat Commun 11, 1169 (2020). https://doi.org/10.1038/s41467-020-14976-9

6. Helena Todorov, Robrecht Cannoodt, Wouter Saelens, Yvan Saeys, TinGa: fast and flexible trajectory inference with Growing Neural Gas, Bioinformatics, Volume 36, Issue Supplement_1, July 2020, Pages i66–i74, https://doi.org/10.1093/bioinformatics/btaa463

7. Tran TN, Bader GD (2020) Tempora: Cell trajectory inference using time-series single-cell RNA sequencing data. PLoS Comput Biol 16(9): e1008205. https://doi.org/10.1371/journal.pcbi.1008205

8. Blasi, T., Hennig, H., Summers, H. et al. Label-free cell cycle analysis for high-throughput imaging flow cytometry. Nat Commun 7, 10256 (2016). https://doi.org/10.1038/ncomms10256

9. Eulenberg P, Köhler N, Blasi T, Filby A, Carpenter AE, Rees P, Theis FJ, Wolf FA. Reconstructing cell cycle and disease progression using deep learning. Nat Commun. 2017 Sep 6;8(1):463. doi: 10.1038/s41467-017-00623-3. PMID: 28878212; PMCID: PMC5587733.

10. Bastidas-Ponce, A. et al. Comprehensive single cell mRNA profiling reveals a detailed roadmap for pancreatic endocrinegenesis. Development 146, (2019).

Reviewers' Comments:

Reviewer #1:
None

Reviewer #2:
Remarks to the Author:
The authors have systemically and methodically answered the questions I raised and appeared to have a similarly good job of replying to the other referees. I am happy to now recommend publication of this manuscript.

Reviewer #3:
Remarks to the Author:
Review of revised VIA manuscript:

R3.Q1: For the synthetic datasets, I am satisfied with the extra metrics that the authors included in the paper, and merged into their final composite metric, that in my opinion, allows a better comparison of the trajectories returned by the different tools.

For the real datasets, I value the addition of the correlation scores for common lineages. While I understand the authors choice not to rely on a fixed trajectory in real datasets (since we can never be completely sure of what the real topology is in those datasets), I nevertheless think that reusing the metrics that they defined for synthetic datasets might have been interesting on real datasets as well.

R3.Q2: The authors answered my concern

R3.Q3: The authors answered my question

R3.Q4: I now agree with the way the authors rephrased the paragraph

R3.Q5: I now agree with the way the authors describe and explain how a starting point can be defined for the VIA method.

R3.Q6 and Q7: The extra experiments that the authors conducted (especially on real datasets) and that are now presented in supplementary figures answer the remaining questions I had.

Manuscript ID: NCOMMS-21-04939B
Author responses to the Final Revisions

Reviewer #2 (Remarks to the Author):
The authors have systemically and methodically answered the questions I raised and appeared to have a similarly good job of replying to the other referees. I am happy to now recommend publication of this manuscript.

We are delighted to see that the Reviewer is satisfied with the revisions and would like to take this opportunity to thank them for their constructive and very thoughtful feedback which led to an improved manuscript.

Reviewer #3 (Remarks to the Author):
R3.Q1: For the synthetic datasets, I am satisfied with the extra metrics that the authors included in the paper, and merged into their final composite metric, that in my opinion, allows a better comparison of the trajectories returned by the different tools.
For the real datasets, I value the addition of the correlation scores for common lineages. While I understand the authors' choice not to rely on a fixed trajectory in real datasets (since we can never be completely sure of what the real topology is in those datasets), I nevertheless think that reusing the metrics that they defined for synthetic datasets might have been interesting on real datasets as well.

We are grateful that the Reviewer appreciates our approach of using the composite metric for offering a more holistic comparison of different trajectories. We agree that the addition of metrics spanning topology and pseudotime have been a critical and necessary improvement to the validation of VIA and thank you for suggesting this. We note your recommendation to apply (perhaps with some modifications) this methodology towards assessing the topologies of real datasets. As part of our future work on VIA, we are considering extending the current composite accuracy framework so it can be applied to real data by formulating a reliable reference topology for the different datasets.

R3.Q2: The authors answered my concern
R3.Q3: The authors answered my question
R3.Q4: I now agree with the way the authors rephrased the paragraph
R3.Q5: I now agree with the way the authors describe and explain how a starting point can be defined for the VIA method.
R3.Q6 and Q7: The extra experiments that the authors conducted (especially on real datasets) and that are now presented in supplementary figures answer the remaining questions I had.

Questions 2-7: We would like to take this opportunity here to thank you for making time to evaluate all the revisions and providing suggestions that have strengthened the manuscript as well as the underlying VIA method.